Atomic Spectroscopy

July/August 2004 Volume 25, No. 4

In This Issue:

ASPND7 25(4) 157–196 (2004)
ISSN 0195-5373

Issues also available electronically.

(see inside back cover)

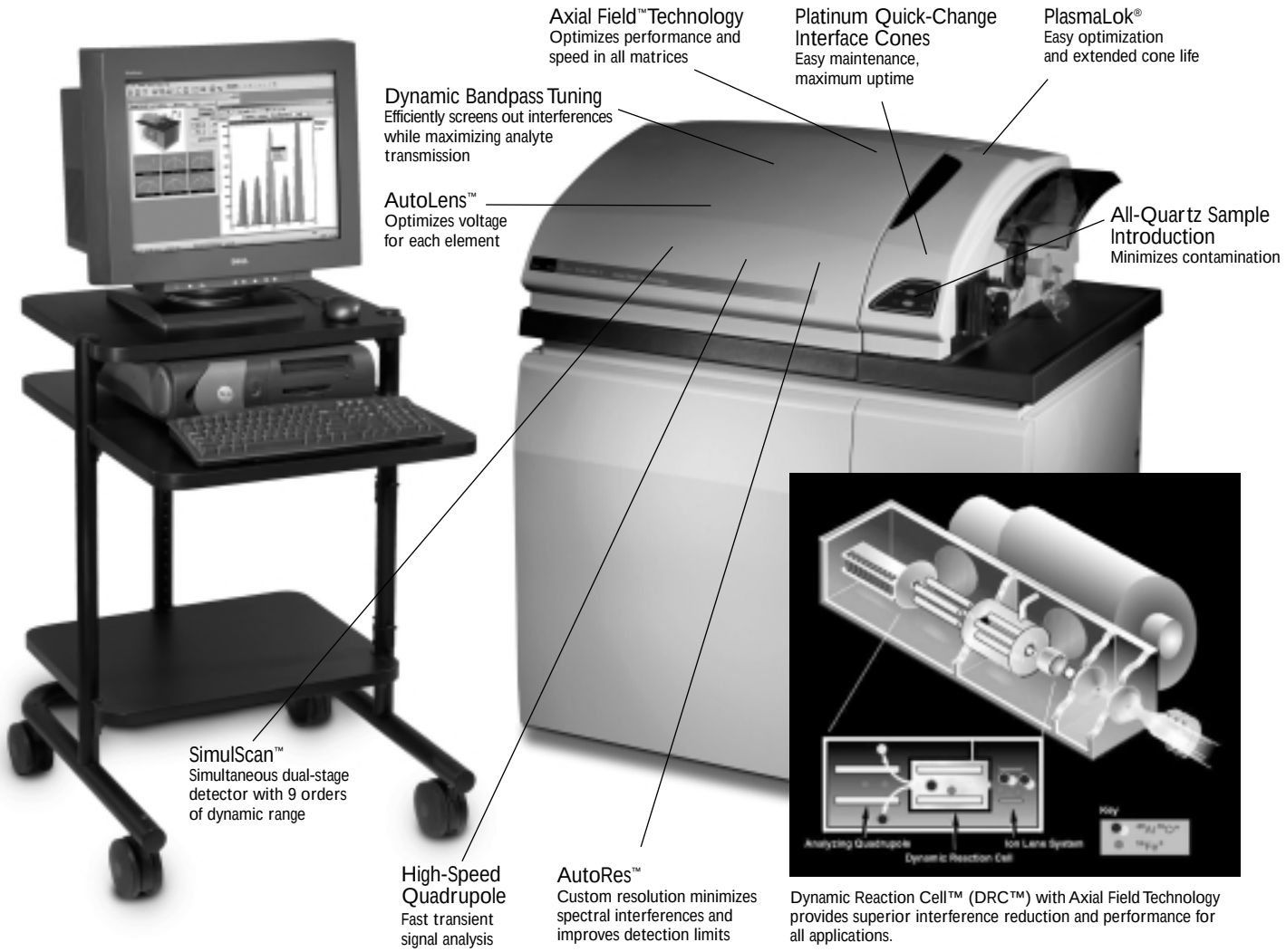

Dynamic Reaction Cell™ (DRC™) with Axial Field Technology provides superior interference reduction and performance for all applications.

Eliminates interferences **COMPLETELY**

When your applications extend beyond the capabilities of conventional ICP-MS, you need the power of the innovative ELAN® DRC II. The DRC II combines the power of patented Dynamic Reaction Cell (DRC) technology with performance-enhancing Axial Field Technology, providing uncompromised sensitivity and performance in all matrices for even the toughest applications. Unlike collision cell, high-resolution, or cold plasma systems, the DRC II completely eliminates polyatomic interferences providing ultratrace-level detection limits.

The DRC II uses chemical resolution to eliminate plasma-based polyatomic species before they reach the quadrupole mass spectrometer. This ion-molecule chemistry uses a gas to “chemically scrub” polyatomic or isobaric species from the ion beam before they enter the analyzer, resulting in improved detection limits for elements such as Fe, Ca, K, Mg, As, Se, Cr, and V.

Unlike more simplistic collision cells, patented DRC technology not only reduces the primary interference; it eliminates sequential side reactions that create new interferences. Unless kept in check by DRC technology, these uncontrolled reactions increase spectral complexity and create unexpected interferences.

PerkinElmer®
precisely.

Determination of Elemental Composition of Zr-Nb Alloys by Glow Discharge Quadrupole Mass Spectrometry

Raparthi Shekhar[a], *J. Arunachalam[a], G. Radha Krishna[b], H.R. Ravindra[b], and B. Gopalan[b]

[a] National Centre for Compositional Characterization of Materials
Bhabha Atomic Research Centre, ECIL Post, Hyderabad 500062, India

[b] Control Laboratory, Nuclear Fuel Complex, ECIL Post, Hyderabad 500062, India

ABSTRACT

The simultaneous determination of trace elements and niobium in Zr-Nb alloys with varying niobium concentrations has been carried out by Glow Discharge Quadrupole Mass Spectrometry (GD-QMS). The Relative Sensitivity Factors (RSF) for the analytes were generated using a certified reference material of a zirconium alloy (zircaloy, non-similar matrix composition). GD-QMS results have been found to be in good agreement with the certified concentrations for several elements of other zirconium-based certified reference materials (zirconium metal and alloys).

This technique is a viable alternative to validate conventional atomic emission and other spectrometric techniques used for the determination of impurities in zirconium-based alloys. With the optimized discharge conditions and pre-sputtering time, the precision of measurements achieved were typically 1% RSD for the majority of elements present at mg kg^{-1} levels, 10% RSD for µg kg^{-1} levels, 0.05% RSD for zirconium (matrix), and 0.05% RSD for niobium (alloying element).

The detection limits for the analytes were found to be at sub-ppm levels with an integration time of 20 ms, 140 points, and four repetitive scans. Molecular interferences observed due to oxygen, matrix, and argon are also listed.

INTRODUCTION

Zr-Nb alloys with varying niobium compositions have been widely used in nuclear technology due to their excellent corrosion-resistant properties and higher mechanical strength than conventional and ternary zirconium alloys (1). While the Zr-2.5%Nb alloy is the preferred structural material for pressure tubes of CANDU type Pressurised Heavy Water Reactors, Zr-1%Nb is used as a fuel cladding material in Pressurised Water Reactors. In view of these important applications, assessment of chemical purity, especially in the determination of trace elements, is of importance. The content of the alloying element niobium, which enhances the mechanical strength and creep-resistance properties of the virgin metal, is present within a narrow concentration range and is also required to be accurately determined. The allowed specifications are 2.5 ± 0.3% in Zr-2.5%Nb alloys and 1.0 ± 0.1% in Zr-1%Nb alloys.

A wide range of analytical methods such as (chemical) Differencial Spectrophotometry (2,3), X-ray Fluorescence Spectrometry (XRFS) (4), DC-Arc Emission Spectrography (DC Arc ES), Inductively Coupled Plasma Optical Emission Spectrometry (ICP-OES), Inductively Coupled Plasma Mass Spectrometry (ICP-MS), and the electro-analytical techniques are employed routinely for the determination of niobium content and the concentrations of other trace elements in Zr-Nb alloys. However, these methods involve tedious matrix separation procedures to determine impurities at trace levels.

*Corresponding author.
E-mail: aruncccm@rediffmail.com

The Differential Spectrophotometric method used for the estimation of niobium at higher concentrations involves the formation of a yellow niobium peroxide complex in concentrated sulphuric acid. This metal yields somewhat lesser sensitivities. However, a molar absorbtivity of $\varepsilon = 1 \times 10^3$ is adequate for the determination of niobium at percentage levels. XRFS is the method of choice for the quick estimation of the major constituents, with suitable reference materials for calibration. However, for the determination of trace constituents in the presence of matrix, XRFS is not quite suitable due to poor sensitivity. The main problem in the emission spectrometric analysis of zirconium and its alloys is the undesirable line-rich emission spectrum of zirconium which leads to spectral interferences (5). In addition, in emission spectrometric methods, the practical detection limits achieved for some elements (like boron) are not adequate for quantification in sub-ppm levels (6). In ICP-MS there is a limitation on the total matrix content, which cannot exceed 0.1–0.2% for effective nebulization. Hence, multiple dilutions are required. Also, the use of HF in dissolution is restrictive with respect to routine use.

GD-QMS offers the advantage of multielement analysis (major, minor, trace, and ultratrace levels) in a single run and exhibits a low matrix dependence for trace elemental analysis of solids. With glow discharge, the sample acts as a cathode, and neutral atoms are sputtered from the surface of the sample and then ionized in the plasma by penning ionization and/or electron impact ionization (7). In GD-MS, the quantification requires the generation of RSF values using suitable solid reference materials. In addition, due to the stability of the plasma, GDMS is superior to the traditionally used spark source mass spectrometry (SSMS) for the analysis of solids and offers a better precision for quanti-

tative analysis. Again, the quantitative separation of zirconium from other trace and ultratrace elements requires multiple solvent extraction steps which are highly tedious and time-consuming, which is obviated in direct solid sample analysis.

Application of GDMS to determine the elemental composition has been reported (8) only for zircaloy NBS standards by generating the RSF values on other zircaloy NBS standards of similar composition. We had reported earlier on the use of GD-QMS for the determination of specific (single) elements such as tin (9), chlorine (10), and boron (6) in zirconium-based alloys.

In the present work, a detailed study has been made on the multielement analysis of zirconium, Zr-Nb, and other zirconium alloys for matrix and trace elements by GD-QMS. The discharge conditions, stabilization time for GD signal and the possible isobaric interferences on isotopes of various analytes are reported. A comparison of the GD-QMS results with those obtained from DC Arc OES, as well as with certified values of elements in Zr-Nb alloys and zirconium metal standards, and other zircaloy standard samples, are presented.

EXPERIMENTAL

Instrumentation

A quadrupole GD-MS, Model GQ230 (VG Elemental, U.K.), was used for the present work. The instrumental parameters are listed in Table I. This instrument was located in our Ultra Trace Analysis Laboratory, inside a class 200 clean room. The discharge was operated in current mode where the discharge voltage was adjusted by changing the flow rate of argon gas using a gas inlet valve. The discharge gas was argon (99.9999% purity); which was additionally purified with an on-line active metal getter. The system interlock gate was operated using compressed argon gas (65 psi) of 99.9995% purity.

The dual detector system (Model No.4870V, Galileo Electro-Optics Corp., USA) utilizes an electron multiplier for ion counting for trace elements (ion currents < 1 x 10^6 ions sec^{-1}) and a Faraday cup for measurement of major and minor elements (ion currents > 1 x 10^6 ions sec^{-1}). The detector system provides a dynamic range of more than eight orders of magnitude, i.e., $1x10^1 – 1x10^{10}$ ions sec^{-1}. Control of instrument and data acquisition was handled by Glo-Quad software. The peak jump mode was used for the data acquisition. A 10-mm anode opening diameter flat sample holder was used. The GD cell in the instrument was cryogenically cooled with liquid nitrogen in order to minimize residual gaseous contaminants.

Mass Calibration

A high-speed stainless steel (HSS) disc containing major elements ranging from carbon (m/z=12) to tungsten (m/z=184) as constituents was chosen for the mass calibration. A small amount of solder (tin-lead alloy) material was also embedded into the HSS sample surface to add Sn (mid mass range ~ 120 amu) and Pb (higher mass ~ 208 amu) masses as well to obtain a more linear mass calibration over the entire mass range.

TABLE I
Instrumental Operating Parameters

Discharge Voltage	1.2 kV
Discharge Current	3.0 mA
Argon flow rate	23.3 sccm
Temperature during discharge	–166ºC
Vacuum (at the quadrupole region)	1 x 10^{-6} mbar
Resolution	300 M/ΔM

Collector Calibration

Collector calibration was done on a daily basis. The Faraday cup and Electron Multiplier detectors were cross-calibrated by measuring the signal intensity at mass 76 ($^{40}Ar^{36}Ar^+$). Detector calibration factor was adjusted to be 2560+200 by adjusting the HT voltage to the electron multiplier before the scanning. The collector calibration was done using a mass step of 0.01 amu and 120 points in peak scan.

Procedure

Sample Preparation for GD-QMS

The surface of different Zr-Nb alloy samples, zircalloy standard samples, and zirconium metal samples were polished to 300 grit with a belt grinder, cleaned with methanol, and then dried under an infrared lamp. Individual samples were loaded into the GD system and degassed under vacuum (around 1 x 10^{-3} mbar) prior to analysis for the removal of atmospheric contaminants. The discharge parameters were optimized to obtain maximum intensity in the form of counts per second (6 x 10^5 ions sec^{-1}) for $^{90}Zr^+$. The sample surface was etched with the plasma at a discharge voltage of 1.2 kV and a current of 3.0 mA for 40 minutes in order to eliminate the initial embedded surface contaminants and obtain a constant standing signal.

The analytical measurements were carried out at a mass step of 0.01 amu with 140 points. A single scan of the Faraday detector for major and minor elements and 20 scans of the electron multiplier for trace and ultratrace elements were used. Four repetitive measurements were recorded.

RESULTS AND DISCUSSION

Discharge Parameters

The studies (11) of the influence of discharge current on the ion

yield indicated that the optimum discharge current is 3.0 mA (with a discharge voltage of 1.0 kV). The 3.0 mA current results in a maximum ion beam intensity, the lowest level of atmospheric and gas-matrix combinations, and a drastically reduced contribution of molecular species (e.g., matrix dimers, etc.). Thus, the discharge current was fixed at 3.0 mA using constant current mode. The discharge voltage at 1.2 kV compared to 1.0 kV resulted in a maximum ion intensity for $^{90}Zr^+$ ion. In our earlier studies (10), the use of 1.2 kV and 3.0 mA gave good results for chlorine in Zr-2.5%Nb alloys. Therefore, discharge conditions of 1.2 kV and 3.0 mA were used for all samples.

Studies on Stabilization Time

Pre-sputtering of the sample (surface) was carried out at the discharge parameters described above. A separate experiment was carried out to determine the actual stabilization time required for the GD signal with respect to elimination of surface contaminants in GD-QMS. The raw counts of some of the common contaminant elements (Na, Mg, Si, Ca) were recorded and converted into ion beam ratios (IBR). The ion beam ratio values were obtained by computing the ratio of raw counts of each isotope normalized to 100% to the abundance normalized raw counts of $^{90}Zr^+$ ion. These IBRs were plotted against each pre-sputter time in Figure 1. The figure reveals that the contamination originating from the sample surface was removed by plasma etching within 35–40 minutes. The GD signal stability was achieved after 40 minutes. Therefore, each sample was pre-sputtered for 40 minutes and the quantitative measurements were made after 40 minutes.

Quantification

Accurate quantitative results in GD-QMS would require the generation of matrix-matched RSF values calculated from certified reference samples with the same or similar composition of the sample to be analyzed. But certified reference materials with the same or similar composition for Zr-Nb alloys for trace and ultratrace levels are not available. Hence, a different composition zirconium alloy matrix (zircaloy, Teledyn standard ZrX868-16D; major elements: Zr, Sn, Fe, Cr) standard, in which several elements were certified, was used for the generation of RSF values for all of its certified elements. Table II lists the RSF values and IBRs for all certified elements. The usability of these RSF values for the determination of elemental concentrations in zirconium metals and Zr-Nb alloys containing different niobium concentrations was investigated.

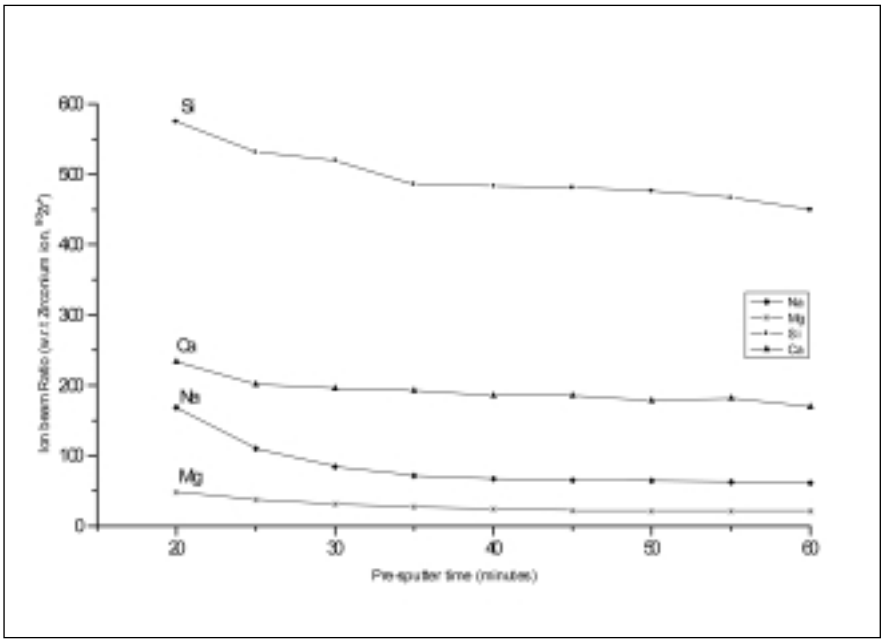

Fig. 1. Dependence of GD signal on pre-sputter time.

Usability of RSF Values

The RSF values for certified elements were generated using their corresponding IBR measured in the zircaloy standard by GD-QMS. These RSF values were applied to IBR values of each Zr-Nb ingot sample and other zirconium standards. The quantitative results so obtained for several elements are listed in Tables III–VI, which provide a comparison of the results for Zr-Nb alloys obtained by GD-QMS against DC Arc-OES and the certified concentrations.

Table III shows that GD-QMS values are in very good agreement with the certified values for the elements Si, P, Ti, V, Cr, Cu, Zr, Nb, Mo, Sn, Hf, Pb, Ca, and Cd in the ZrX869-25B standard and for the elements P, Ti, V, Cr, Mn, Fe, Ni, Cu, Zr, Nb, Mo, Hf, Ca, Cd in the ZrX867-16D standard. Somewhat higher values compared to the corresponding certified values for the elements Co, Ta, W, Na, and Mg (in the ZrX869-25B standard) and for Si, Co, Sn, Ta, W, Na, and Mg (in the ZrX867-16D standard) were obtained by GD-QMS. The GD values were lower compared to the corresponding certified values for the elements Mn, Fe, Ni in ZrX869-25B standard and Pb in ZrX867-16D standard. These (minor) disagree-

TABLE II
Relative Sensitivity Factors Generated Using ZircaloyTeledyn Std. (Zrx868-16D) Certified Values by GD-QMS

Elements	Zircaloy Teledyn Std. Zrx868-16D Certified Values (mg kg^{-1})	GD-QMS Ion Beam Ratios (mg kg^{-1})	RSF Value Generated
^{30}Si	179±4	471±15	0.380
^{31}P	35±3	49±2	0.712
^{49}Ti	122±16	400±7	0.305
^{51}V	93±5	303±7	0.307
^{52}Cr	580±26	521±5	1.114
^{55}Mn	56±2	52±1	1.087
^{56}Fe	2787±66	4198±51	0.665
^{60}Ni	134±6	165±2	0.209
^{59}Co	42±1	61±1	0.686
^{63}Cu	83±2	17±0.4	4.755
^{90}Zr	98.709%	98.847±0.017%	1.000
^{93}Nb	570±12	550±14	1.037
^{98}Mo	128±2	66±2	1.948
^{119}Sn	1.23±0.03%	0.228±0.006%	5.413
^{178}Hf	178±6	66±1	2.716
^{181}Ta	716±4	181±2	3.959
^{182}W	112±13	24±0.2	4.596
^{208}Pb	101±11	8.4±0.3	12.035
^{23}Na	<10	64±3	<0.156
^{24}Mg	<5	22±1	<0.224
^{44}Ca	<10	283+ 3	<0.009
^{114}Cd	<0.2	56±2	<0.004

ments noted may be due to the compromised optimised conditions used for the determination of many elements. Hence, certain deviations were seen with respect to the certified concentrations. The results shown in Tables IV and V indicate that there is good agreement for GD values with the certified values of hafnium in zirconium metals and zircalloys, and also for indicated values of the elements in the zirconium metals and zircalloy standards. Tables VI and VII indicate that the RSFs generated provide fairly accurate values for the elements (Cr, Fe, Ni, Cu, Nb, Sn) in Zr-2.5%Nb samples and (P, Ti, Cr, Mn, Fe, Ni, Cu, Nb, Mo, Cd, Sn, Hf, Pb, Ca) in Zr-1%Nb alloys in comparison to DC Arc AES values. The agreement seen reveals that the computed RSF values from zircaloy standard (non similar matrix composition) are quite applicable to zirconium based samples such as pure metal as well as Zr-Nb alloys with varying niobium concentrations.

In our earlier study of tin (9) analysis by GD-QMS, we found that the RSF value of tin in zirconium matrix (zircaloy) was 1.39 and 4.93 at liquid nitrogen temperatures (i.e., with cooling the sample) and ambient temperature (i.e., without cooling the sample), respectively, at a discharge voltage of 1.1 kV and 1.0 mA. In the present study, the RSF value of tin in zirconium matrix was 5.413 at discharge voltage of 1.2 kV and 3.0 mA at liquid nitrogen temperatures. The change in RSF values with respect to the discharge parameters is being investigated.

Spectral Interferences

Some of the dominant molecular ionic species noted in the GD-QMS spectrum of the zirconium matrix are given in Figure 2. The interference from the Zr^{+2} (Figure 2a) ion species significantly affects the determination of Sc and Ti (^{45}Sc, ^{46}Ti, ^{47}Ti, and ^{48}Ti). Hence, ^{49}Ti was used for quantification of titanium. Molecular ionic species formed by oxides and argides with the matrix are interfering with the elements Pd, Ag, Cd, Sn (mass numbers: 106,107, 108, 110, 112; Figure 2b) and Xe, Ba (mass numbers: 130, 131, 132, 134, 136; Figure 2c), respectively. Other isobaric interferences due to argon gas are observed: $^{40}Ar^{+4}$, $^{40}Ar^{+3}$, $^{40}Ar^{+2}$, $^{40}Ar^{36}Ar^{+}$, $^{40}Ar_2^{+}$, and $^{40}Ar_3^{+}$.

Analytical Precision

Tables III–VII also show internal reproducibility of the determinations in the Zr-Nb alloy samples at trace and ultratrace levels. The uncertainties in these estimates are expressed as overall standard deviations, and the computed % RSDs are based on multiple measurements under the given discharge conditions (n=4). The overall precision for the determination of analytes was typically 1% RSD for the majority of the elements present at mg kg^{-1} levels, 10% RSD for µg kg^{-1} levels, 0.05% RSD for zirconium (matrix), and 0.05% RSD for niobium (alloying element). These data are indicative of the stability of the GD plasma during the measurements and the degree of homogeneity of the sample at trace and ultratrace levels in the alloy.

Atomic Spectroscopy
Vol. 25(4), July/August 2004

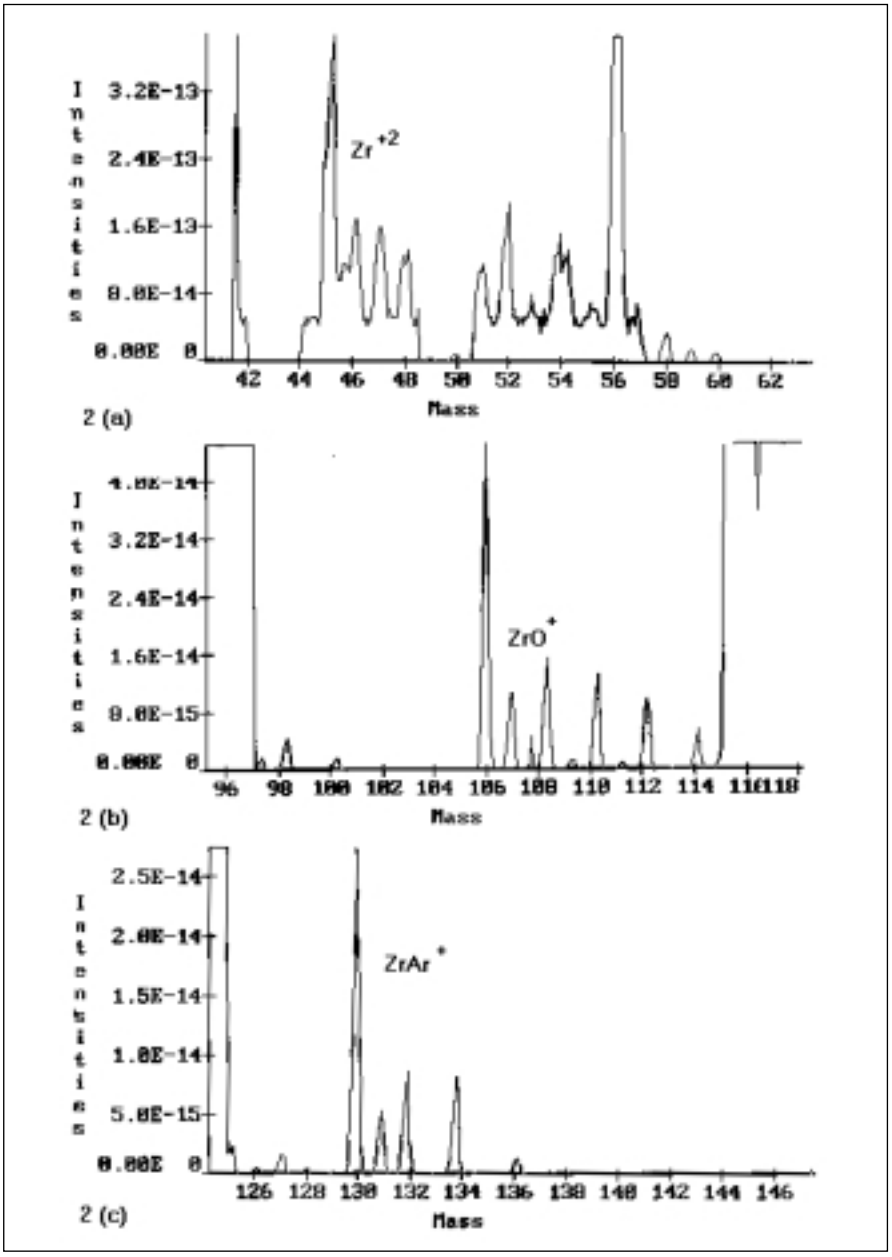

Fig. 2 (a,b,c). Molecular ionic species observed in the GD-QM Spectrum of Zr.

Detection Limits

Unlike other spectrometric techniques, in GD-QMS the blank (baseline) signal cannot be measured independently without the sample. In our measurements, each isotope region is measured using 140 points across with a mass step of 0.01 amu. The total width of the scanning window is about 1.4 amu of which 0.8 amu in the center is integrated as the signal for the isotope. The signal for the baseline is measured at the wings of each peak. The detection limit in our case was defined as three times the standard deviation of this background signal (12), based on multiple scans (n=4), which is converted into the corresponding concentration value using the computed concentration of the element (isotope). For most of the analytes, the detection limits were found to be in the sub-ppm levels.

CONCLUSION

The sensitivity offered by GD-QMS enables the accurate determination of trace constituents in Zr and Zr-Nb based alloys at concentration levels much lower than their specified levels. This, in turn, enables assessment of the efficiency of the manufacturing processes.

This study provides such an assessment of the Zr-Nb alloy samples manufactured indigenously. Even though GD-MS is not available as a routine analytical technique in many laboratories, an assessment of the measurement accuracy by other analytical techniques with different physico-chemical principles with a technique capable of direct analysis would better enable quality improvement steps implemented in bulk production of critical components such as nuclear-grade zirconium metal and alloys.

TABLE III
Comparison of GD-QMS Concentrations With Certified Values of Zircaloy Teledyne Standards

Elements	Zircaloy Teledyn Std Zrx869-25B Certified Values (mg kg^{-1})	GD-QMS (mg kg^{-1})	Zircaloy Teledyn Std. Zrx867-16D Certified Values (mg kg^{-1})	GD-QMS (mg kg^{-1})
Si	94±10	93±1	31±3	59±1.5
P	49±8	38±0.6	102±7	112±2.1
Ti	55±1	55±0.01	19±4	17±0.4
V	47±4	42±0.2	20±1	17±3
Cr	1057±32	991±22	1630±26	1630±10
Mn	54±1	44±0.4	6±1	5±0.1
Fe	2247±35	2090±10	1630±40	1640±20
Ni	68±5	30±3	33±3	34±1
Co	17±1	23±0.09	10±1	18±0.6
Cu	36±1	37±0.3	8±1	7±0.2
Zr	97.872%	97.799±0.016%	97.604%	97.186±0.029%
Nb	276±16	263±2.4	102±10	96±1.5
Mo	59±1	53±0.4	10±1	11±0.3
Sn	1.65±0.03%	1.681±0.018%	2.00±0.02%	2.344±0.026%
Hf	77±4	85±1.3	31±3	36±0.5
Ta	396±5	442±5	207±7	241±4
W	46±9	60±0.9	23±2	39±0.7
Pb	44±1	47±0.7	16±1	8.0±0.2
Na	<10	<24	<10	<59
Mg	<5	<16	<5	<32
Ca	<10	<5	<10	<9
Cd	<0.2	<0.25	<0.2	<0.35

TABLE IV
Comparison of GD-QMS Concentrations With Indicated Values of NBS Zirconium Metal Standards

Elements	Zr Metal NBS Std 1234 Indicated (by NBS) Values (mg kg^{-1})	GD-QMS (mg kg^{-1})	Zr Metal NBS Std 1236 Indicated (by NBS) Values (mg kg^{-1})	GD-QMS (mg kg^{-1})
Si	40	69±1	205	192±9
P	7	10±0.2	19	30±0.4
Ti	20	19±0.6	185	206±1.3
V	5	6±0.2	20	70±0.7
Cr	55	110±2.3	250	355±12
Mn	10	23±0.6	45	46±0.1
Fe	240	385±15	1700	1630±20
Ni	20	16±0.8	140	127±2.6
Co	5	23±0.09	50	39±0.2
Cu	<10	35±0.5	250	243±0.9
Zr	99.837%	99.858±0.016%	99.288%	99.461±0.006%
Nb	55	42±1.3	600	606±4.5
Mo	2	15±0.6	100	120±1.0
Sn	15	16±0.9	60	104±4
Hf	46±3*	45±2	198±6*	181±7
Ta	85	95±5	700	668±16
W	25	27±1.4	140	188±5
Pb	5	10±0.8	25	46±1

* Certified value.

Atomic Spectroscopy
Vol. 25(4), July/August 2004

TABLE V
Comparison of GD-QMS Concentrations With Indicated Values of NBS Zircaloy Standards

Elements	Zr Metal NBS Std 1237 Indicated (by NBS) Values (mg kg^{-1})	Zr Metal NBS Std 1237 GD-QMS (mg kg^{-1})	Zr Metal NBS Std 1238 Indicated (by NBS) Values (mg kg^{-1})	Zr Metal NBS Std 1238 GD-QMS (mg kg^{-1})	Zr Metal NBS Std 1239 Indicated (by NBS) Values (mg kg^{-1})	Zr Metal NBS Std 1239 GD-QMS (mg kg^{-1})
Si	35	66±3	170	90±0.1	95	130±2
P	62	125±4	20	31±2.3	26	50±0.8
Ti	30	21±0.7	100	101±3.3	40	75±1.3
V	10	23±0.7	25	72±1.8	15	56±0.8
Cr	1510	1770±40	580	636±7.6	1055	1120±10
Mn	10	9±0.4	60	50±1.3	50	54±0.8
Fe	1650	1640±30	2500	2630±80	2300	2160±30
Ni	40	24±0.7	100	94±2.3	45	30±0.5
Co	10	15±0.5	40	32±0.6	15	24±0.5
Cu	<10	8.5±0.2	60	37±0.3	30	45±1
Zr	97.616%	97.059±0.114%	97.957%	98.304±0.056%	97.776%	96.647±0.042%
Nb	85	105±2.5	550	483±11	220	261±5
Mo	<10	12±0.6	120	99±1.4	45	57±2
Sn	1.9%	2.476±0.109%	1.26%	1.040±0.045%	1.61%	2.785%±0.043%
Hf	31±3*	37±1.6	178 + 6*	140±4.0	77±4*	84±2.5
Ta	200	226±8	700	547±15	400	413±12
W	25	33±1.5	95	88±0.6	45	57±0.3
Pb	15	14±0.7	80	78±1.5	30	46±2

* Certified value.

TABLE VI
Comparison of GD-QMS Concentrations With Chemical Values in Zr-2.5% Nb Alloy Coolant Tube Samples

Elements	Zr-2.5% Nb Sample No. 1 DC Arc OES (mg kg^{-1})	Zr-2.5% Nb Sample No. 1 GD-QMS (mg kg^{-1})	Zr-2.5% Nb Sample No. 2 DC Arc OES (mg kg^{-1})	Zr-2.5% Nb Sample No. 2 GD-QMS (mg kg^{-1})
Cr	150	128±5	160	149±4
Fe	700	648±99	810	757±3
Ni	<70	19±2	< 70	20±1
Cu	<30	10±0.2	< 30	4.7±0.1
Nb*	2.6%	2.856±0.007%	2.6%	2.637±0.025%
Sn	29	21±1	42	26±1

DC Arc OES: DC Arc Optical Emission Spectrographic method.
* : Analyzed by X-Ray Fluorescence Spectrometric method.

ACKNOWLEGMENTS

The authors thank Dr. J.P. Mittal, Director, Chemistry and Isotope Group, BARC, and Shri P.S.A. Narayanan, DCE (QA, MS & C), NFC, for their encouragement and constant support in carrying out the present work.

Received July 31, 2003.

TABLE VII
Comparison of GD-QMS Concentrations With Chemical Values of Zr-1% Nb Alloy Samples

Elements	Zr-1%Nb Sample No. 1		Zr-1%Nb Sample No. 2		Zr-1%Nb Sample No. 3		Zr-1%Nb Sample No. 4		Zr-1%Nb Sample No. 5	
	DC Arc AES	GD-QMS	DC Arc AES	GD-QMS	DC Arc AES	GD-QMS	DC Arc AES	GD-QMS	DC Arc AES	GD-QMS
	(mg kg^{-1})		(mg kg^{-1})		(mg kg^{-1})		(mg kg^{-1})		(mg kg^{-1})	
P	< 10	3.9±0.1	< 10	7.7±0.2	< 10	4.7±0.1	< 10	8.7±1.4	< 10	4.3±0.2
Ti	< 25	5.0±0.1	< 25	9.9±0.3	< 25	14±0.3	< 25	5.7±0.1	< 25	6.0±0.3
Cr	<100	86±8	<100	111±2	<100	108±2	<100	88±1	<100	93±7
Mn	24	20±0.3	27	24±0.2	27	26±0.6	26	24±0.4	29	26±2
Fe	280	306±10	305	328±8	275	338±7	325	329±12	315	301±7
Ni	< 70	20±0.2	< 70	24±1	< 70	24±1	< 70	13±4	< 70	15±1
Cu	< 30	6.9±0.3	< 30	9.6±0.2	< 30	8.4±0.3	< 30	12±0.2	< 30	29±1
Nb*	1.08	1.135± 0.009%	1.1%	1.158± 0.005%	1.1%	1.116± 0.004%	1.1%	1.102± 0.005%	1.1%	1.137± 0.037%
Mo	< 25	0.90±0.05	< 25	1.0±0.05	< 25	1.2±0.1	< 25	0.91±0.01	< 25	0.88+0.05
Cd	< 0.3	<0.01	< 0.3	<0.76	< 0.3	<0.01	< 0.3	<0.8	< 0.3	<0.01
Sn	< 25	6.6±0.3	< 25	7.2±0.7	< 25	7.6±0.8	< 25	7.9±0.7	< 25	6.9±0.3
Hf	< 50	16±0.4	< 50	14±0.2	< 50	15±0.8	< 50	15±0.3	< 50	15±0.7
Pb	< 25	8.5±0.2	< 25	7.3±0.3	< 25	7.7±0.8	< 25	8.4±1.2	< 25	9.5±0.1
Ca	<25	6.3±0.2	<25	4.7±0.9	<25	4.5±0.1	<25	4.0±0.1	<25	3.2±0.1

DC Arc OES: DC Arc Optical Emission Spectrographic method .
* : Analyzed by X-Ray Fluorescence Spectrometric method.

REFERENCES

1. K.N. Choo, Y.H. Kang, S.I. Pyun, and V.F. Urbanic, Journal of Nuclear Materials 209, 226 (1994).
2. M. Schafei and F. Schutle, Z. Anal. Chem. 149, 73 (1956).
3. G. Scharlot and J. Saulnier, Chim. Anal. (Paris), 35, 51 (1953).
4. H.R. Ravindra, G. Radhakrishna, R. Narayan Swamy, and B. Gopalan, Estimation of Niobium in Zr-Nb alloys by X-ray Spectrometry, Proceedings of the National Workshop on "Testing and Characterisation of Materials," TACOM-90, held at Mumbai, India, 15-16th March, 1990, edited by E. Ramadasan, p.198–208 (1990).
5. I. Steffan and G. Vujicic, JAAS 9, 785 (1994).
6. Raparthi Shekhar, J. Arunachalam, G. Radha Krishna, H.R. Ravindra, and B. Gopalan, Determination of Boron at parts per billion levels in Zr-Nb alloys by Glow Discharge Quadrupole Mass Spectrometry. Communicated to 14th International Symposium on Zirconium in the Nuclear Industry, sponsored by the ASTM Committee B10 on Reactive and Refractory Metals and Alloys. Date of symposium: June 13-17, 2004, Stockholm, Sweden.
7. W.W. Harrison, K.R. Hess, R.K. Marcus, and J.L. King, Anal. Chem. 58(2), 341 (1986).
8. Keith Robinson and Edward F.H. Hall, Glow Discharge Mass Spectrometry for Nuclear Materials, Journal of Metals, April, 1987, p.14-16, Testing and Analysis.
9. R. Shekhar and J. Arunachalam, GD-QMS Analysis of Tin in Zirconium Alloy Matrix, p.686, 8th ISMAS Symposium on Mass Spectrometry, held December 7–9, 1999, at Hyderabad, India.
10. R. Shekhar, J. Arunachalam, H.R. Ravindra, and B. Gopalan, J. Anal. At. Spectrom.18, 381 (2003).
11. GloQuad system Manual for Fisons Instruments (VG Elemental), Issue 2.0 (1993).
12. Laura Aldave de las Heras, Erich Hrnecek, Olivier Bildstein, and Maria Betti, J. Anal. At. Spectrom. 1011-1014, 17 (2002).

The Determination of Gold in Ore Samples by Inductively Coupled Plasma Optical Emission Spectrometry(ICP-OES)

***K. Chandra Sekhar[a], K.K. Gupta[b], S. Bhattacharya[b], and S. Chakravarthy[b]**

[a] Analytical Chemistry and Environmental Sciences, Discovery Lab, Indian Institute of Chemical Technology (IICT), Hyderabad, 500 007, India

[b] Analytical Chemistry Division, National Metallurgical Laboratory, Jamshedpur 831 007, India

ABSTRACT

Fire assay is the most common technique for the determination of precious metals in rock and ore samples, and is generally accurate for the determination of gold. However, with the development of modern laboratory techniques such as Inductively Coupled Plasma-Optical Emission Spectrometry (ICP-OES) and Inductively Coupled Plasma-Mass Spectrometry (ICP-MS), alternative methods have become available which offer the advantages of rapid determination of small concentrations of gold in a number of samples for preliminary exploration studies.

A multi-parametric linear regression model was used to estimate the observed interferences and using this model, the gold content in ores has been estimated.

A simple analytical method for the determination of gold in ore samples using ICP-OES is reported and these results show that this method can be successfully applied when the gold concentration is high (above 0.7ppm) with an error in the range of 9–11% in ore samples. The advantage of this method over conventionally adopted Fire Assay is small sample size and larger sample throughput.

INTRODUCTION

Accurate analyses of exploration data and ore reserves are two of the most important functions of professional geologists and engineers in mine development. The problems encountered become particularly acute when dealing with precious metal values. Fire assay (1,2) has been and remains the most common technique for the determination of precious metals in rock and ore samples. The accuracy of the fire assay technique is satisfactory for the analysis of the vast majority of precious metal-bearing ores. Recoveries, micro-analytical observations (3), and uninterrupted use without basic modifications for more than 2,000 years (4) attest to that fact. One basic reason for the continued use of the fire assay technique is its ability to analyze relatively large sample size that can be treated by this technique; another reason is that fire assay is relatively free of interferences (5).

However, there are problems associated with the fire assay method which are complex and not very well understood. The examples of high recovery rates, in some cases of apparently more than 100%, and the results obtained in micro-analytical studies both indicate that there can be inaccuracies. Inductively coupled plasma optical emission spectrometry (ICP-OES) is a powerful and time-saving method with multielement capabilities.

Taking advantage of this, an attempt has been made to use this technique for the determination of gold in a number of ore samples from Purulia, West Bengal, India, for pre-exploration studies without prior separation of the matrix.

**Corresponding author*
current address: Analytical Chemistry Group, Defence Metallurgical Research Laboratory (DMRL), Kanchanbagh, Hyderabad (A.P.), India
E-mail: kavi@iict.ap.nic.in or kavi223@yahoo.com

EXPERIMENTAL

Instrumentationl

A Shimadzu GVM-1014P (Japan) vacuum ICP-OES was used for analysis of the samples. A Varian Ultra Mass 700 (Victoria, Australia) ICP-MS was used for interlaboratory comparison.

Reagents and Standards

All metal solutions used in this study were prepared from Johnson-Matthey SpecPure (San Diego, California, USA) samples. Two standard reference materials of gold from CANMET (Toronto, Ontario, Canada) were used for validation and calibration purposes.

Measurements

The measurements were performed using the gold emission line at 242.2 nm. Initial experiments were carried out using 1 ppm of gold to optimize the instrumental parameters. The optimum instrumental parameters selected for this study are listed in Table I. The methodology was validated with gold ore standards and applied for the determination of gold-bearing ores from Purulia, West Bengal. One gram gold ore was digested in 15 mL HNO_3, the silica was removed by adding HF acid, and gold was subsequently taken into solution by aqua regia.

Interference Study

The analytical protocol for the determination of gold ore was established with synthetically prepared solutions of gold, and the most likely interferents such as W, Mn, Ti, Cr, Fe, Ta, and Pt. A semi-quantitative analysis was carried

TABLE I
Instrumental Parameters for ICP Study

RF power	1.2 KW
Argon flow rates	
-- Outer gas	16 L/min
-- Intermediate gas	0.4 L/min
-- Carrier gas	1.2 L/min
-- Purge (argon) gas	4 L/min
Observation height	15 mm
Focal length	1000 mm
Polychromator	Paschen Runge mounting
Linear dispersion	0.467 nm/mm
Exit slit	30 µm

out for 30 elements in gold ore samples of Purulia, WB, to establish their abundance (Table II) in the ore samples.

Each of these 30 elements (pure synthetic solutions) was aspirated and measurements were made at the gold wavelength of 242.2 nm to establish whether these elements contribute to spectral interferences (Table III). Out of 30 elements studied, 12 elements were found to give substantial background intensity (above 0.1) at 242.2 nm compared to gold intensity of 0.36125. The concentration of Ca and V is high in ore samples, but their intensity at the gold emission line is very low (approximately 0.104) and are considered not important. Even though the concentration of Cu (H to L), Ni (H to UT), and Al (H to L) varies from low to high concentrations, their intensity at the gold wavelength is negligible (below 0.16), much lower than the gold intensity (0.36125) and, hence, these elements are not considered for interference studies. The remaining seven elements were identified as significant elements as the concentration of Fe, Cr, Mn, and W was high (see Table II) and the background intensity of Ti, Ta, and Pt is substantial (see Table III).

TABLE II
List of Probable Interferents and Their Abundances in Gold Ores from Purulia, West Bengal

1. Ag	T	11. Ga	UT	21. Se	UT
2. Al	H to L	12. Mg	H	22. Si	H to T
3. As	A	13. Mn	H	23. Sn	A
4. Bi	A	14. Mo	UT	24. Ta	T to UT
5. Ca	H	15. Nb	A	25. Te	A
6. Cd	A	16. Ni	H to UT	26. Ti	H to T
7. Co	UT	17. P	H to T	27. U	H to L
8. Cr	H	18. Pb	UT	28. W	H to UT
9. Cu	H to L	19. Pt	L to UT	29. Zn	UT
10. Fe	H	20. Sb	A	30. Zr	A

H: High (100 ppm and above) L: Low (10-100 ppm)
T: Trace (1-10 ppm) UT: Ultra Trace (Below 1 ppm)
A: Absent

TABLE III
List of Elements Studied at Gold Wavelength (242.2nm) and Their Emission Intensities

Blank	**0.10070**	**Au**	**0.36125**
Cu (1000ppm)	0.16085	Ta (10ppm)	0.13060
Mn (50ppm)	0.21995	Ti (1000ppm)	0.10395
Mg (100ppm)	0.10360	Ca (100ppm)	0.10360
Cr (1000ppm)	0.13570	W (100ppm)	0.13040
Ni (1000ppm)	0.10116	Fe (1000ppm)	0.15385
Al (1000ppm)	0.10090	Pt (100ppm)	0.10590

The objective of this investigation was to study the effect of these seven matrix elements (Fe, Cr, Mn, W, Ti, Ta, and Pt) on gold estimation. All solutions were prepared in 5% (v/v) HNO_3. The concentration (ppm) ranges of the sample matrix elements were maintained as follows:
W = 0–100 ppm; Mn = 0–50 ppm;
Ti = 0–50 ppm; Cr = 0–50 ppm;
Fe = 0–250 ppm; Ta = 0–10 ppm;
Pt = 0–10 ppm.

These concentrations were chosen to cover the wide variations in ore samples obtained from Purilia (see Table II). The effect of individual interferents on the analyte signal obtained from the binary solutions was used to predict the total interference effect on the gold signal (Table IV). Every measured value was an average of five replicate measurements and was found to be within ± 2σ. Table IV represents a typical binary mixture (6x6) of Fe–Au showing the set of concentrations (in ppm) in which Fe–Au solutions were prepared. For example, a binary solution of Fe–Au, solution No. 15 (Table IV) contains 1 ppm of gold and 50 ppm of iron in the binary mixture. The other binary systems, such as Mn–Au and W–Au, were prepared in a similar manner in order to compute the coefficients.

TABLE IV
Example of Synthetic Binary Mixture Used in Interference Study*

	0 ppm Au	0.5 ppm Au	1.0 ppm Au	2.0 ppm Au	4.0 ppm Au	8.0 ppm Au
	Sol. No.	Sol. No.	Sol. No.	Sol. No.	Sol. No.	Sol. No.
0 ppm Fe	1	2	3	4	5	6
25 ppm Fe	7	8	9	10	11	12
50 ppm Fe	13	14	15	16	17	18
100 ppm Fe	19	20	21	22	23	24
200 ppm Fe	25	26	27	28	29	30
250 ppm Fe	31	32	33	34	35	36

**Each solution contains Fe-Au, I.e., solution No. 15 contains 1 ppm Au and 50 ppm Fe.*

RESULTS AND DISCUSSION

Spectral Interferences

The spectral interference from these seven (Fe, Cr, Mn, W, Ti, Ta and Pt) accompanying concomitants (Table III) on the intensities of gold was investigated. A calibration curve was drawn for each of these seven elements at the gold wavelength and their intensities were plotted against 1 ppm pure gold to arrive at the gold equivalent concentration. This is the concentration that is recorded by the concomitants other than the gold concentration (Table V).

From Table V it can be see that these seven matrix elements will give a substantial emission intensity signal at the gold emission line ranging from 0.017 ppm (for Pt) to 0.456 ppm (for Mn) even at low concentrations (10–50 ppm). A software program was developed to calculate the gold equivalents for each of the concomitants and to establish the total gold equivalent. The true gold value was obtained by substracting the total gold equivalent from the net gold concentration.

Chemical Interferences

Computational elimination of interelement interferences has received much attention recently because of its simplicity and practical utility. In this study, we used a simple mathematical model for the interference study proposed originally by Thompson et al. (6) and Pszonicki (7,8).

Interference of a major constituent on a trace analyte can be considered due to two components: either independent of or dependent on the trace analyte concentration (Figure I). Line 'a' is the calibration curve for the pure element (analyte). Line 'b' represents a parallel shift in the calibration curve due to interference. This is known as a 'translational' effect and is independent of analyte concentration. Such interference in ICP is obtained because of a background. Curves 'c' and 'd' represent, respectively, linear and non-linear 'rotational' shifts of the calibration curves. In both cases, the analyte signal is a function of both analyte and interferent concentrations. Rotational shift of the calibration curve, being a function of both analyte and interferent concentrations, may be expressed as:

$$y_a = y_t \cdot f(x) \qquad \text{(Eq. 1)}$$

where y_a and y_t are, respectively, the apparent and true concentrations of the analyte and f(x) is a function of the interferent concentrations, x. Assuming f(x) to be a linear function of x, one can write:

$$y_a = y_t \cdot (Ax+C) \qquad \text{(Eq. 2)}$$

TABLE V
Apparent Gold Concentrations of the Interferents Present in Purulia Ore Samples

Element	Conc. (ppm)	Apparent Gold Conc. (ppm)
W	100	0.0450
Mn	50	0.4557
Ti	50	0.0050
Cr	50	0.0050
Fe	250	0.0755
Ta	10	0.1010
Pt	10	0.0166

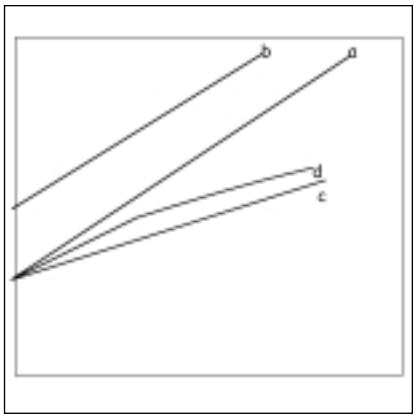

Fig. 1. Different types of interferences: (a) calibration curve with pure component, (b) translational effect, (c) linear rotational effect, and (d) non-linear rotational effect.

It is evident from Equation 1 that at x = 0, f(x) = 1, which indicates that there is no interference at all. Equation 2 may then be rewritten as:

$$y_a = y_t \cdot (Ax+1) \qquad \text{(Eq. 3)}$$

Similarly, the translational effect, being independent of analyte concentration, may be expressed as:

$$y_a = y_t + f(x) \qquad \text{(Eq. 4)}$$

where y_a, y_t and f(x) bear the same meaning as stated before. Assuming f(x) to be a linear function of x, Equation 4 may be rewritten as :

$$y_a = y_t + (Bx+C) \qquad \text{(Eq. 5)}$$

As stated before, at x=0 f(x)=0, there is no interference at all. Equation 5 may be rewritten as:

$$y_a = y_t + Bx \qquad \text{(Eq. 6)}$$

combining rotational and translational effects:

$$y_a = y_t (1+Ax) + Bx \qquad \text{(Eq. 7)}$$

Thompson et al. (6) calculated coefficients A and B (the characteristic coefficients representing the binary analyte-interferent pair under consideration) by a graphical method. In this work, A and B are calculated from a linear regression of Equation 7 for every analyte-interferent pair. These coefficients serve as characteristic coefficients for calculating the interference effect in a multicomponent system. For such a system, Equation 7 may be generalized as :

$$y_a = y_t (1+ \sum_i A_i x_i) + \sum_i B_i x_i \qquad \text{(Eq. 8)}$$

where 'i' is the number of interferents; x_i is the concentration of the i^{th} interferent, and A_i; B_i the characteristic coefficients for the pertinent analyte interferent pair. Equation 8 may be rearranged to predict the true analyte concentration:

$$yi = \frac{y_a - \sum_i B_i x_i}{1+ \sum_i A_i x_i} \qquad \text{(Eq. 9)}$$

The characteristic coefficients (A and B for every binary, gold-interferent pair) were found by linear regression analysis.

Analytical Application

To verify the applicability of the proposed model, three synthetic mixtures were prepared. Calibration curves for gold and inherent elements (Fe, Cr, Mn, W, Ti, Ta, and Pt) were prepared taking solutions of pure gold and matrix elements. The concentrations of gold and of the interferent present in the synthetic mixture were estimated using the calibration curves prepared earlier. The apparent gold concentrations thus obtained from the pure gold calibration curve were subjected to the computational correction for interference using the coefficients A and B. The corrected gold concentrations agreed well with the known gold concentration in the synthetic solutions. Table VI shows the apparent and corrected concentrations of gold using the coefficients A and B.

From Table VI it is clear that the corrected values are within the range of experimental error and in good agreement with the true values. The performance of the present model is therefore considered satisfactory.

Six real samples were analyzed for gold using the above model and the results are shown in Table VII. The corrected values are in good agreement with the fire assay values in the case of the first three samples (Sample No. 1 to Sample No. 3) and standards (Sample No. 8 to Sample No.11). In the case of the remaining samples (Sample No. 4 to Sample No. 7), the corrected values are satisfactory and give an approximation of the gold concentration, which will help in carrying out pre-exploratory studies. This variation may be due to the low concentration of gold and the complex nature of the ore sample.

TABLE VI
Analysis of Synthetic Solutions Using the Interference Correction Model

Synthetic Solutions	Concentrations in ppm							Gold (ppm)	
	W	Mn	Ti	Cr	Fe	Ta	Pt	Added	Found
1S	25.0	25.0	0.0	5.0	50.0	5.0	1.0	0.02	0.03
*	21.4	27.3	0.0	5.4	54.5	3.9	1.5	–	–
#	0.01	0.23	0.0	0.0	0.01	0.02	0.0	–	–
2S	5.00	5.00	0.0	12.5	100.0	2.5	2.5	0.20	0.25
*	4.80	5.60	0.0	108.3	2.1	2.95	–	–	
#	0.0	0.05	0.0	0.0	0.03	0.02	0.0	–	–
3S	50.00	25.0	0.0	25.0	125.0	1.0	5.0	0.20	0.16
*	45.2	25.7	0.0	24.90	124.7	1.5	5.5	–	–
#	0.03	0.22	0.0	0.0	0.03	0.02	0.01	–	–

* Indicates the concentration of the concomitants found.

# Indicates the corresponding gold equivalent.

Atomic Spectroscopy
Vol. 25(4), July/August 2004

TABLE VII
Analysis of Real Samples
Using the Interference Correction Model

Sample No.	Sample	Gold Content (ppm)	
		Fire Assay	ICP-OES (After Correction)
1.	Ghatsila conc	3.0	2.67
2.	Ghatsila Tails	0.10	0.20
3.	M/9731	0.70	0.70
4.	KM/142	1.20	2.80
5.	BC/322	0.10	1.21
6.	KB/166	0.08	0.14
7.	B/7604	0.04	0.36
8.	CANMET-MA-1b (Certified Value: 17ppm)	16.8	18.00
9.	CANMET-MA-2b (Certified Value: 2.39ppm)	2.41	2.25
10.	OX-12 (Certified Value: 6.6ppm	6.36	8.13
11.	OX-11 (Certified Value: 2.94ppm	3.02	3.42

CONCLUSION

Fire assay is the most accurate method for the determination of gold. However, with the development of instrumental techniques like ICP-OES, alternative methods have become available which may offer the advantage of rapid determination of gold and also the advantage of the analysis of a number of samples. The results for the gold analysis from the present method are in good agreement with Fire Assay results when the gold concentration is high (above 0.7ppm). The results for gold standards are very much in good agreement with certified values and this may be due to the fact that the matrix composition is known and a proper correction factor can be applied. In the case of low gold concentration in the ores, the error is very high and this method gives an approximate value of gold present in the ore samples. This method is very useful for pre-exploratory studies where sample number and time of analysis is important. This is not possible with Fire Assay as this method is time-consuming, requires large sample size, and is not environmentally safe.

Revision received April 23, 2004.

REFERENCES

1. E.E. Bugbee, A textbook of Fire assaying, The Colorado School of Mining Press, Golden, Colorado, USA (1981).
2. E.A. Smith, The sampling and assaying of the precious metals, Met-Chem Research, Inc., Boulder, Colorado, USA (1987).
3. C. Gasparrinni, Gold and other precious metals-the lure and the trap (first published in 1989), the Space Eagle Publishing Company Inc., Toronto, Canada and Tucson, Arizona, USA. The second revised edition was printed by Springer Verlag, Heidelberg, Germany (1991).
4. C.Gasparrini, Mining Magazine, July 1993, 31-35
5. W.G. Bacon, G.W. Hawthorn, and G.W. Poling, CIM Bulletin, p. 29 (Nov. 1989).
6. M. Thompson, S.J. Waltin, and S.J. Wood, Analyst 104, 299 (1979).
7. L. Pszonicki, Talanta 24, 613 (1977).
8. L. Pszonick and A. Lkszo-Bienkowska, Talanta 24, 617 (1977).

Determination of Cadmium at the Nanogram per Liter Level in Seawater by Graphite Furnace AAS Using Cloud Point Extraction

Chun-gang Yuan, *Gui-bin Jiang, Ya-qi Cai, Bin He, and Jing-fu Liu
Key Laboratory of Environmental Chemistry and Ecotoxicology
Research Center for Eco-Environmental Sciences, Chinese Academy of Sciences
P. O. Box 2871, 100085 Beijing, P.R. China

ABSTRACT

A method based on cloud point extraction was developed to determine cadmium at the nanogram per liter level in seawater by graphite furnace atomic absorption spectrometry. Diethyldithiocarbamate (DDTC) was used as the chelating reagent to form Cd-DDTC complex; Triton X-114 was added as the surfactant. The parameters affecting sensitivity and extraction efficiency (i.e., pH of the solution, concentration of DDTC and Triton X-114, equilibration temperature, and centrifugation time) were evaluated and optimized. Under the optimum conditions, a preconcentration factor of 51.6 was obtained for a 20-mL water sample. The detection limit was as low as 2.0 ng L^{-1} and the analytical curve was linear in the 10.0–200.0 ng L^{-1} range with satisfactory precision (RSD <4.7%). The proposed method was successfully applied to the trace determination of cadmium in seawater.

INTRODUCTION

It is well known that cadmium can accumulate in human organs and cause serious diseases such as cancer, hypercalciuria, and the very painful illness called itai-itai ('ouch-ouch') disease (1). Genotoxical studies show that cadmium acts as an inhibitor of DNA mismatch repair in yeast (2). In a recent rat study, it was reported that cadmium can also act as an estrogen mimic and exert adverse effects on the estrogen-responsive tissues of the uterus and the mammary glands (3). These study results have drawn renewed attention to the pollution and toxic effects of cadmium, and will contribute in revising the regulatory standards for cadmium exposure. Because of the generally low concentration levels of cadmium in nature, noticeable adverse effects to the environment and human beings are very low. It is therefore very important to develop effective analytical methods for the trace level determination of cadmium in samples with complex matrices. To investigate cadmium concentrations at the ppb or ppt levels, graphite furnace atomic absorption spectrometry (GFAAS) is one of the most favored choices. Unfortunately, the determination of cadmium in seawater is difficult even with GFAAS, equipped with Zeeman-effect background correction, not only due to the low Cd levels in the samples but also due to the severe interferences caused by high-salinity matrices. To decrease matrix interferences during GFAAS analysis, different kinds of atomizers (4–8) have been developed. Although these types of atomizers are effective to some extent, they are not available in many laboratories for routine analysis. The use of chemical matrix modifiers is another way to decrease the interferences from the matrix (9,10), but it is not usually adequate for seawater sample analysis. In this case, some sample pretreatment (preconcentration and separation from matrices) including electrolysis (11), coprecipitation (12), liquid–liquid extraction (LLE) (13–16), and solid-phase extraction (SPE) (17–21) is necessary before routine determination of cadmium at the nanogram per liter level in seawater with ordinary graphite tubes. Unfortunately, all of these methods require a large sample volume and they are time-consuming. In particular, the traditional liquid–liquid extraction method is not only time-consuming and labor-intensive but is also dangerous to analysts because of the large volume of volatile organic solvent required.

As a green liquid–liquid extraction method, cloud point extraction (CPE) has been employed in analytical chemistry to separate and preconcentrate organic compounds (22–24) and metal ions (25–29). Compared with the traditional organic liquid–liquid extraction, cloud point extraction requires a very small amount of relatively nonflammable and nonvolatile surfactants that are benign to the environment. Aqueous solutions of non-ionic surfactants may separate in two phases in a narrow temperature range, called the cloud point. Using appropriate conditions such as temperature, pressure, and pH value, the solution containing the surfactant becomes turbid and separates into a surfactant-rich phase (in very small volume) and the remaining larger volume (bulk amount) into the diluted aqueous solution with the surfactant concentration, which is approximately equal to its critical micelle concentration (CMC). The hydrophobic analytes of the solution are extracted into the surfactant-rich phase. Since the surfactant-rich phase volume is very small in com-

*Corresponding author.
e-mail: gbjiang@mail.rcees.ac.cn
Tel: 8610-62849334
Fax: 8610-62849179

parison to the initial solution volume, a high enrichment factor can be obtained.

Pinto et al. (25) reported using 1-(2-pyridylazo)-2-naphthol (PAN) and Chen et al. (27) used 1-(2-thiazolylazo)-2-naphthol (TAN) as the chelating reagent with Triton® X-114 as the surfactant to extract ultratrace cadmium in seawater after cloud point extraction. The determination was performed using flame atomic absorption spectrometry. Although higher enrichment factors were achieved, the concentration of cadmium in seawater was too low to be compatible for the detection limit capability of a FAAS system. Cadmium determination at the nanogram per liter levels in seawater samples has only been successfully performed by complexing O,O-diethyl-dithiophosphate (DDTP) with cadmium, followed by cloud point extraction and ultrasonic nebulization inductively coupled plasma mass spectrometry (ICP-MS) (30).

In the present study, a method was developed for the trace level determination of cadmium (ng L^{-1} level) in seawater employing cloud point extraction coupled with GFAAS using diethyldithiocarbamate (DDTC) as the chelating reagent and Triton X-114 as the surfactant. The results obtained after extraction show that cadmium was determined successfully, with satisfactory recoveries and precision.

EXPERIMENTAL

Instrumentation

A Hitachi Z-5700 atomic absorption spectrometer (Hitachi High-Technologies Corporation, Japan), equipped with Zeeman background correction and a cadmium hollow-cathode lamp as the radiation source, was used. The working conditions (listed in Table I) were adjusted in accordance with the manufacturer's recommendations. The absorbance signals were measured as peak height with manual injection. A thermostated bath (TB-85 Therma Bath, Shimadsu, Japan), maintained at the desired temperature, was used to obtain cloud point preconcentration. A centrifuge and calibrated centrifuge tubes (Beijing Medicinal Instrument Company, P.R. China) were used to accelerate the phase separation process. The Easypure System (Model D7382-33, Barnstead Thermolyne Corporation, Dubuque, IA, USA) produced the deionized water (18 MΩ) used for this study.

Reagents and Standard Solutions

All reagents used were of analytical grade. Working standard solutions were obtained by appropriate dilution of the stock standard solution (1000 µg mL^{-1}) with distilled water. The non-ionic surfactant Triton X-114 (Acros Organics, New Jersey, USA) was used without further purification. The DDTC aqueous solution was prepared by dissolving appropriate amounts of sodium diethyldithiocarbamate (NaDDTC) (Beijing Chemical Factory, P.R. China) immediately before each experiment.

The materials and vessels used for trace analysis were kept in 10% (v/v) nitric acid for at least 48 h and were subsequently washed four times with deionized water (obtained from the Easypure System) before use.

Cloud Point Extraction Procedure

For the preconcentration of Cd, aliquots of 20.0 mL of the cold sample solution containing the analyte, 1.5 g L^{-1} Triton X-114 and 0.01 g L^{-1} DDTC, buffered at a suitable pH, were mixed and kept for 20 min in the thermostatic bath at 40°C. Then the phase separation was accelerated by centrifugation for 6 min at 3000 rpm. After cooling in an ice-bath for 5 min, the surfactant-rich phase was separated with a syringe. After removing the bulk aqueous phase, the remaining micellar phase (about 100 µL) was treated with 100 µL of the methanol solution of 1% (v/v) nitric acid to reduce its viscosity. Then, 20 µL of the sample was introduced into the GFAAS by manual injection. During the experiment, 10 µL of 200 mg L^{-1} $Pd(NO_3)_2$ of the chemical modifier was applied.

The conventional liquid-liquid extraction of Cd in Cd-DDTC complex form in the samples using CCl_4 was carried out to compare these results with the cloud point extraction method results.

TABLE I
Instrumental Operating Conditions

Lamp Current	9 mA	Cuvette	A-type
Wavelength	228.8 nm	Gas Flow	30 mL min^{-1}
Slit	1.3 nm	Sample Volume	20 µL

Temperature Program

Stage	Temperature (°C)		Ramp Time	Hold Time
	Start	End		
Drying	80	140	40 s	
Ashing	300	300	20 s	
Atomizing	1600	1600		5 s
Cleaning	2000	2000		4 s

Extraction of Cd in Real Samples

The seawater samples were filtered through a 0.45-µm pore size membrane filter to remove the suspended particulate matter and then stored at 4ºC in the dark. A 20-mL sample, adjusted at pH 9 with ammonia and nitric acid, was submitted to the cloud point extraction procedure for preconcentration using 1.5 g L^{-1} Triton X-114 and 0.01 g L^{-1} DDTC. After phase separation, a 100-µL methanol solution containing 1% (v/v) nitric acid was added to the surfactant-rich phase. The treated samples were introduced into the GFAAS by manual injection.

RESULTS AND DISCUSSION

Effect of pH

The extraction efficiency, depending on the pH values at which the cloud point extraction of Cd was performed, was optimized. As an important parameter, the effect of pH on the extraction of Cd was investigated in the 1–13 pH range and the results are illustrated in Figure 1. It was found that the atomic absorbance reached maximum at pH 9, at which point maximum extraction efficiency was obtained. For this study, pH 9 was selected as the working pH.

Effect of DDTC Concentration

In general, the concentration of a chelating reagent has a remarkable influence on the extraction efficiency. In order to select the optimum concentration of DDTC (while keeping other experimental parameters constant), the effect of the concentration of the chelating reagent on the extraction efficiency was examined and the results are presented in Figure 2. It can be seen that maximum signals were obtained at 0.01 g L^{-1} DDTC ($-\log C_{DDTC} = 2$); therefore, 0.01 g L^{-1} DDTC was chosen as the chelating reagent for this study.

Effect of Concentration of Triton X-114

For a successful cloud point extraction procedure, Triton X-114 was chosen for the formation of the surfactant-rich phase due to its low cloud point temperature (23–25ºC) and high density of the surfactant-rich phase (31). The properties of Triton X-114 facilitate the extraction procedure and phase separation by centrifugation. In this experiment, the variation of extraction efficiency upon the surfactant concentration in the 0.1–4.0 g L^{-1} range was investigated and the results are shown in Figure 3. It can be seen that the absorbance signal increased with an increase in concentration of Triton X-114 up to 1.0 g L^{-1}. When the concentration of Triton X-114 was varied between 1.0 and 2.5 g L^{-1}, the signal kept a plateau, which shows that a quantitative extraction by cloud point extraction was obtained. With an increase in Triton X-114 concentration over 2.5 g L^{-1}, the signal decreased because of an increase in the volume and viscosity of the surfactant phase. Based on these experimental results, 1.5 g L^{-1} Triton X-114 was adopted as the optimum amount to achieve best analytical signals and highest extraction efficiency.

Effect of Equilibration Temperature

The best analyte preconcentration factor was achieved when the cloud point extraction procedure was processed at equilibration tem-

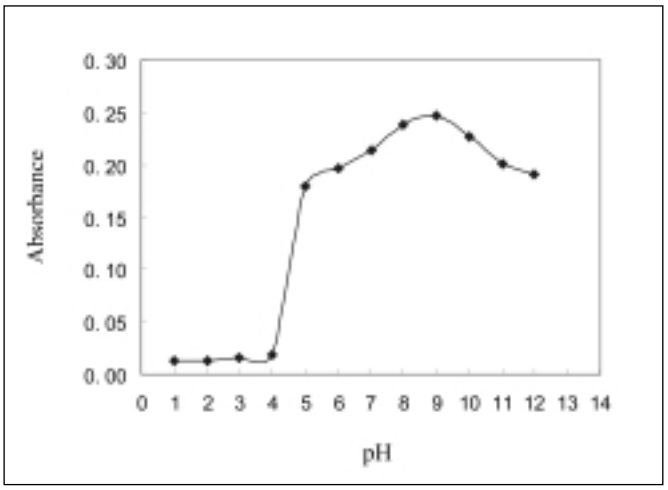

Fig. 1. Effect of pH on preconcentration of Cd. Conditions: 0.20 ng mL^{-1} Cd 20 mL, 0.01 g L^{-1} DDTC, 1.5 g L^{-1} Triton X-114 at 40ºC. Other experimental conditions are described in Cloud point extraction procedure section.

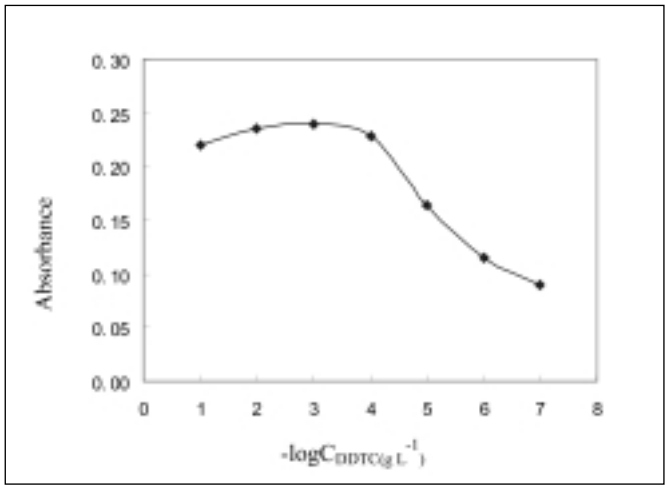

Fig. 2. Influence of DDTC concentration on the absorbance signal of Cd. Conditions: 0.20 ng mL^{-1} Cd 20 mL, pH 9.0, 1.5 g L^{-1} Triton X-114 at 40ºC. Other experimental conditions are described in Cloud point extraction procedure section.

Atomic Spectroscopy
Vol. 25(4), July/August 2004

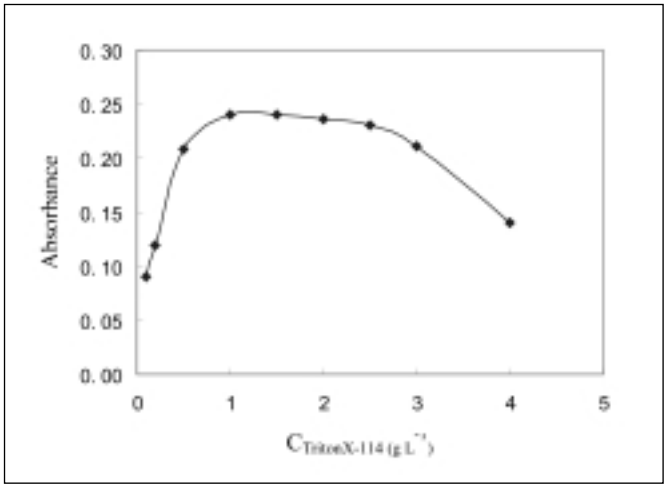

Fig. 3. Variation of the analytical signal of the Cd with Triton X-114 concentrations. Conditions: 0.20 ng mL^{-1} Cd 20 mL, pH 9.0, 0.01 g L^{-1} DDTC at 40ºC. Other experimental conditions are described in Cloud point extraction procedure section.

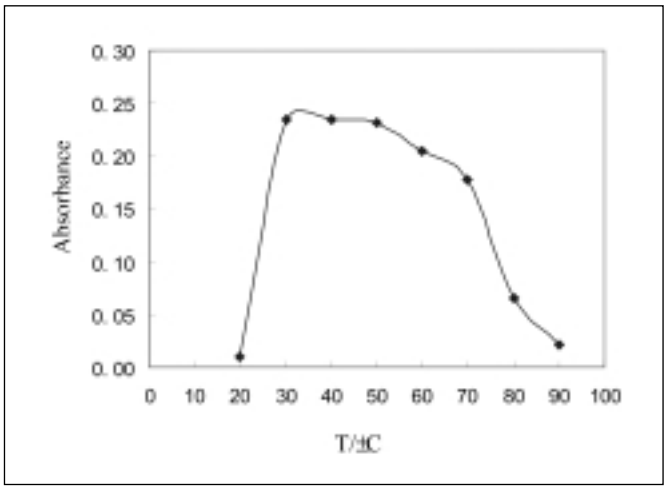

Fig. 4. Effect of equilibration temperature on the analytical signal. Conditions: 0.20 ng mL^{-1} Cd 20 mL, pH 9.0, 0.01 g L^{-1} DDTC, 1.5 g L^{-1} Triton X-114 at 40ºC. Other experimental conditions are described in Cloud point extraction procedure section.

peratures that were well above the cloud point temperature of the surfactant (32). The enrichment factor was also affected by time (33). Thus, it was necessary to examine the effect of temperature on cloud point extraction. In order to employ the shortest incubation time and the lowest possible equilibration temperature, and to ensure the completion of the reaction and the efficient separation of phases, the effects of equilibration temperature and time were examined. Figure 4 shows the effects of equilibration temperature on the absorbance signal. Maximum signals were obtained at temperatures between 30–50ºC. At 20ºC, which was below the cloud point temperature of Triton X-114, two phases cannot be formed and the metal complex cannot be extracted. When the temperature was above 60ºC, the signal decreased due to the decomposition of the Cd-DDTC complex. Therefore, 40ºC was selected as the working equilibration temperature.

The equilibration time was also selected based on the best signal and efficient extraction obtained in the time span between 5–60 min. It was found that an incubation time of 20 min was sufficient for quantitative extraction, and 20 min was subsequently chosen as the equilibration time for our experiments.

Effect of Centrifugation Time

The effect of centrifugation time on extraction efficiency was studied in the time range of 1–30 min at 3000 rev. min^{-1}. The results showed that there were no appreciable improvements time periods longer than 5 min at which complete separation occurred. A centrifugation time of 6 min was therefore selected as optimum.

Figures of Merit

Calibration curves were constructed by preconcentrating 20 mL of standard solutions with 1.5 g L^{-1} Triton X-114. The surfactant-rich phase was diluted with 100 µL of a solution of methanol containing 1% (v/v) nitric acid to reduce its viscosity. Then, 20 µL of diluted solution was introduced into the GFAAS by manual injection. Under the optimum experimental conditions, the calibration curve for Cd was linear from 0.01 to 0.20 ng mL^{-1} with good relative standard deviation (RSD<4.7%) and a detection limit (3δ) (reagent blank, n=6) as low as 0.002 ng mL^{-1} was obtained. Figures of cloud point extraction and conventional liquid-liquid extraction by CCl_4 are compared in Table II. An enrichment factor of 51.6-fold was obtained by preconcentrating a 20-mL solution. Further improvement can be obtained by employing larger amounts of the sample solution or by diluting the surfactant-rich phase to a smaller volume with the methanol solution.

Interferences

Cations that may react with DDTC and anions that may form complexes with cadmium were the two main interferences affecting the preconcentration process. The effects of representative potential interfering species were tested and the results are listed in Table III. The results show that cadmium recoveries were almost quantitative in the presence of most foreign cations, except for Hg^{2+}, Sn^{4+}, Pb^{2+} which led to negative interferences with recoveries of 62.9%, 71.3%, 79.8%, respectively. The absorbance profiles are shown in

TABLE II
Analytical Characteristics of the Different Preconcentration Methods for Cd

Method	Solvent	Enrichment Factor	D.L. (ng mL^{-1})[c]	R.S.D. (%)	Regression Equation	R^2
Without Preconcentration	--	1	0.101	2.7	A=0.026C+0.0056	0.9992
Liquid–liquid Extraction[a]	CCl_4	16.2	0.007	3.9	A=0.4216C+0.0092	0.9945
Cloud-point Extraction[b]	Triton X-114	51.6	0.002	4.7	A=1.3402C+0.0087	0.9961

[a] Sample volume was 100 mL, CCl_4 volume was 5 mL.
[b] Sample volume was 20 mL, Triton X-114 rich phase volume was 0.10 mL.
[c] D.L. means detection limit (3δ) (reagent blank).

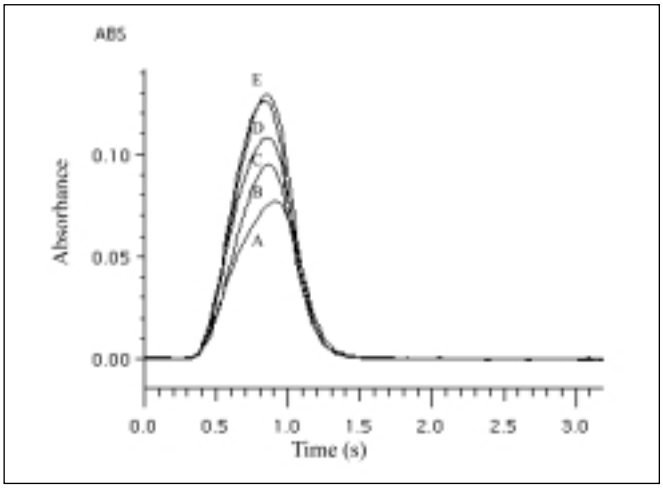

Fig. 5. Absorbance profiles of Cd obtained with and without interferences.
A: 0.10 ng mL^{-1} Cd^{2+} with 1.0 ng mL^{-1} Hg^{2+}, 0.01 g L^{-1} DDTC;
B: 0.10 ng mL^{-1} Cd^{2+} with 5.0 ng mL^{-1} Sn^{4+}, 0.01 g L^{-1} DDTC;
C: 0.10 ng mL^{-1} Cd^{2+} with 5.0 ng mL^{-1} Pb^{2+}, 0.01 g L^{-1} DDTC;
D: 0.10 ng mL^{-1} Cd^{2+} with 1.0 ng $mL^{-1}$$Hg^{2+}$, 5.0 ng mL^{-1} Sn^{4+} and 5.0 ng $mL^{-1}$$Pb^{2+}$, 0.10 g L^{-1} DDTC;
E: Standard solution of 0.10 ng mL^{-1} Cd^{2+} without any interference, 0.01 g L^{-1} DDTC, other conditions in this test are the optimal as described in the text.

Figure 5. The peak shapes were not changed for co-extraction of Hg^{2+}, Sn^{4+}, Pb^{2+} and these interferences can be avoided by employing a higher concentration of DDTC reagent (0.10 g L^{-1}). The results indicated that the interferences by Hg^{2+}, Sn^{4+}, Pb^{2+} resulted mainly from the metal complex formation with DDTC. Under the experiment conditions employed, interferences were not detected in the real samples, resulting in satisfactory recoveries of 84.8–108.9%.

Real Sample Analysis

The method proposed was applied to the determination of Cd in seawater samples to test its reliability and practicality. Six seawater samples from the East China Sea (collected in November 2002) were preconcentrated

TABLE III
Influence of Foreign Ions on the Preconcentration and Determination of Cd*

Foreign Ion	Foreign Ion to Analyte Ratio	Recovery (%)[a]
Cl^-	2.5×10^8	98.1±2.1
SO_4^{2-}	8×10^7	96.7±1.7
HCO_3^-	1×10^4	103.2±3.1
CO_3^{2-}	1×10^4	94.6±1.2
NO_3^-	1×10^4	99.0±3.4
F-	1×10^4	97.7±2.7
Fe^{3+}	2000	98.7.±1.9
Fe^{2+}	2000	95.4±4.2
Zn^{2+}	2000	105.2±3.5
As^{3+}	1000	94.2±1.8
As^{5+}	1000	103.2±2.4
Cr^{6+}	500	102.4±2.9
Cr^{3+}	500	98.5±1.1
Mo^{6+}	500	89.1±2.9
Bi^{3+}	500	97.9±3.4
Cu^{2+}	200	101.8±2.6
Mn^{2+}	100	94.2±3.1
Co^{2+}	50	91.3±0.9
Ni^{2+}	50	99.1±4.1
Pb^{2+}	50	79.8±3.8
Sn^{4+}	50	71.3±2.9
Hg^{2+}	10	62.9±3.7

[a] Mean±standard deviation (95% confidence interval, n=6).
*Preconcentration step: 0.10 ng mL^{-1} Cd^{2+}, pH 9.0, 0.01 g L^{-1} DDTC, 1.5 g L^{-1} Triton X-114 at 40ºC.

by cloud point extraction and analyzed by GFAAS. For this purpose, 20 mL of each water sample was preconcentrated with 1.5 g L^{-1} Triton X-114 and 0.01 g L^{-1} DDTC. The results of the real sample analysis are listed in Table IV. The concentrations of Cd in these samples were in the range of 0.051–0.156 ng mL^{-1}. Recovery tests were carried out with standard cadmium-spiked real seawater samples at three different concentrations. The obtained recoveries (84.8–108.9%) were satisfactory and indicated that the method can be successfully applied to real samples.

CONCLUSION

Compared with conventional liquid–liquid extraction, cloud point extraction (CPE) is a much more environmentally friendly method and is safer for the analysts because of the small volume of innoxious surfactants used in place of toxic organic solvents. The surfactant can be easily introduced into the GFAAS by manual injection after dilution with a methanol solution containing nitric acid. Interferences from anions such as chlorine and humic acid can be avoided since the metal complexes are separated. Under optimum conditions, a preconcentration factor of 51.6 was obtained for a 20-mL water sample. The detection limit was as low as 2.0 ng L^{-1} and the analytical curve was linear in the 10.0–200.0 ng L^{-1} range with satisfactory precision (RSD <4.7%). The proposed method was successfully applied to the trace determination of cadmium in seawater with satisfactory recoveries (84.8–108.9%). The experiment proved that cloud point extraction is a convenient, safe, simple, rapid, and inexpensive preconcentration method for cadmium determination at the nanogram per liter levels in seawater samples, resulting in a high enrichment factor.

TABLE IV
Determination of Cd in Real and Spiked Samples

Sample No.	Location	Measured (ng mL^{-1}) *	Spiked (ng mL^{-1})	Found (ng mL^{-1}) *	Recovery[a] (%)
			0.050	0.110±0.003	118.0
W1	31°59.893’ N; 123°30.195’ E	0.051±0.002	0.085	0.142±0.005	107.1
			0.120	0.163±0.006	93.3
			0.050	0.117±0.004	96.0
W2	31°30.092’ N; 123°00.272’ E	0.069±0.004	0.085	0.149±0.005	94.1
			0.120	0.193±0.003	103.3
			0.050	0.161±0.005	104.0
W3	31°00.460’ N; 122°29.870’ E	0.109±0.005	0.085	0.179±0.007	82.4
			0.120	0.213±0.006	86.7
			0.100	0.241±0.009	85.0
W4	30°41.866’ N; 122°43.798’ E	0.156±0.003	0.150	0.283±0.010	84.7
			0.200	0.312±0.008	78.0
			0.050	0.135±0.004	98.0
W5	30°30.603’ N; 123°29.623’ E	0.086±0.004	0.085	0.176±0.006	105.9
			0.120	0.199±.009	94.2
			0.100	0.219±0.008	98.0
W6	30°00.220’ N; 123°00.507’ E	0.121±0.003	0.150	0.248±0.011	84.7
			0.200	0.286±0.007	82.5

* Mean ± standard deviation (95% confidence interval, n=6).

[a] 100 × [(Found-base)/spiked].

ACKNOWLEDGMENT

This work was jointly supported by the National Natural Science Foundation of P.R. China (20137010, 20205008) and the Chinese Academy of Sciences (KZCX2-414).

Received October 12, 2003.

REFERENCES

1. L. Jarup, Nephrology Dialysis Transplantion 17, 35 (2002).
2. Y.H. Jin, A.B. Clark, R.J.C. Slebos, H. Al-Refai, J.A. Taylor, T.A. Kunkel, M.A. Resnick and D.A. Gordenin, Nature Genetics 34, 326 (2003).
3. M. D. Johnson, N. Kenney, A. Stoica, L. Hilakivi-Clarke, B. Singh, G. Chepko, R. Clarke, P.F. Sholler, A.A. Lirio, C. Foss, R. Reiter, B. Trock, S. Paik and M.B. Martin, Nature Medicine 9, 1081 (2003).
4. K.R. Lum and M. Callaghan, Anal. Chim. Acta 187, 157 (1986).
5. W. Slavin, D.C. Manning, G. Carnrick, and E. Pruszkowska, Spectrochim. Acta Part B 38, 1157 (1983).
6. B.V. L'vov, L.P. Pelieva, and A.N. Sharnopolski, Z. Prikl, Spektrosk. 27, 395 (1977).
7. M.-S. Chan and S.-D. Huang, Talanta 51, 373 (2000).
8. I.L. Grinshtein, Y.A. Vilpan, L.A. Vasilieva, and V.A. Kopeikin, Spectrochim. Acta Part B 54, 745 (1999).
9. J.Y. Cabon, Spectrochim. Acta Part B 57, 513 (2002).
10. S. Sachsenberg, T. Klenke, W.E. Krumbein, H.J. Schellnhuber, and E. Zeeck, Anal. Chim. Acta 279, 241 (1993).
11. W. Lund and B. V. Larsen, Anal. Chim. Acta 72, 57 (1974).
12. E. A. Boyle and J. M. Edmond, Anal. Chim. Acta 91, 189 (1977).
13. R. Guevremont , R.E. Sturgeon, and S.S. Berman, Anal. Chim. Acta 115, 163(1980).
14. R. G. Smith, Jr., and H. L. Windom, Anal. Chim. Acta 113, 39 (1980).
15. D. Cossa, G. Canuel, and J. Piuze, Marine Chem. 12, 224 (1983).
16. P. J. Statham, Anal. Chim. Acta 169, 149 (1985).
17. Z.R. Xu, H.Y. Pan, S.K. Xu, and Z.L. Fang, Spectrochim. Acta Part B 55, 213 (2000).
18. D. Colbert, K.S. Johnson, and K.H. Coale, Anal. Chim. Acta 377, 255 (1998).
19. P.G. Su and S.D. Huang, Anal. Chim. Acta 376, 305 (1998).
20. R. Ma and F. Adams, Anal. Chim. Acta 317, 215 (1995).
21. M.H. Wang, A.I. Yuzefovsky, and R.G. Michel, Microchem. Journal 48, 326 (1993).
22. D.S. Bai, J.L. Li, S.B. Chen, and B.H. Chen, Environmental Science and Technology 35, 3936 (2001).
23. I. Casero, D. Sicilia, S. Rubio, and D. Pérez-Bendito, Anal. Chem. 71, 4519 (1999).
24. R. Carabias-Martínez, E. Rodríguez-Gonzalo, J. Domínguez-Alvarez, and J. Hernández-Méndez, Anal. Chem. 71, 2468 (1999).
25. C.G. Pinto, J. L. P. Pavón, B. M. Cordero, E. R. Beato, and S. G. Sánchez, J. Anal. At. Spectrom. 11, 37 (1996).
26. S. Akita, M. Rovira, A.M. Sastre, and H. Takeuchi, Separation Science and Technology 33, 2159(1998).
27. J. Chen and K.C. Teo, Anal. Chim. Acta 434, 325 (2001).
28. D.L. Giokas, E.K. Paleologos, and M.I. Karayannis, Analytical Bioanalytical Chemistry 373, 237 (2002).
29. J.L. Manzoori and G. Karim-Nezhad, Anal. Chim. Acta 484, 155 (2003).
30. M.A.M. de Silva, V.L.A. Fescura, and A.J. Curtius, Spectrochim. Acta Part B 55, 803 (2000).
31. W.L. Hinze and E. Pramauro, Critical Reviews in Analytical Chemistry 24, 133 (1993).
32. P. Frankewich and W.L. Hinze, Anal. Chem. 66, 944 (1994).
33. D.A. Johnson and T.M. Florence, Anal. Chim. Acta 53, 73 (1971).

Monitoring of Cd, Cr, Cu, Fe, Mn, Pb and Zn in Fine Uruguayan Wines by Atomic Absorption Spectroscopy

Mario E. Rivero Huguet
Analytical Chemistry Department, Trace Elements Area, LATU
Laboratorio Tecnológico del Uruguay
Av Italia 6201, CP 11500, Montevideo, Uruguay

ABSTRACT

Metals in wine occur at the mg/L level or even less and, though not directly related to the taste of the final product, their content should be determined because excess is undesirable and in some cases restricted by legislation to guarantee consumer health protection.

Seven elements were determined in 14 white and 33 red wines from nine Uruguayan wineries.

Several techniques have been approved for the determination of metallic ions in wine, but the most sensitive and rapid is atomic absorption spectroscopy.

In the present work, flame atomic absorption spectrometry (FAAS) was employed for the determination of Cu, Fe, Mn, and Zn, and graphite furnace-atomic absorption spectrometry (GF-AAS) was used for Cd, Cr, and Pb determination.

The following concentration (mg/L) ranges were obtained for Cd (0.002–0.003), Cr (0.004–0.052), Pb (0.006–0.057), Cu (0.034–0.65), Fe (0.73–4.6), Mn (0.74–2.2), and Zn (0.49–2.2). Mean recoveries of elements from fortified wines were: 98.3±2.6% for Cd, 101.5±1.7% for Cr, 99.1±2.7% for Pb, 96.9±1.4% for Cu, 97.3±3.1% for Fe, 98.1±1.9% for Mn and 95.7±3.8% for Zn. The detection limits (mg/L) were: 0.0005 for Cd, 0.001 for Cr, 0.003 for Pb, 0.006 for Cu, 0.020 for Fe, 0.008 for Mn and 0.007 for Zn.

The concentrations of all the metal ions analyzed in wines fall within the range typical of wines from around the world and none of them is above the limits established by the Office International de la Vigne et du Vin (OIV).

INTRODUCTION

Wine quality is affected by several factors. Historically, the expertise of the sage winemaster was used to gauge the quality of the product. Nowadays, many environmental concerns, health factors, and governmental rules prompt the producers of fine wines to monitor several important components in the grape must, the fermentation vats, and in the final wine.

One of them is the content of metallic ions. The knowledge of metal content in wine is used to identify the geographic region in which the grapes were grown and the type of pesticide applied as well. It also enables to assure some of the organoleptic characteristics of wine and to carry on close control of the toxic metals content in the final product (1–14).

As a way to control the metal ions in wine, some countries have imposed rules restricting metal content in wines. These rules must be followed by the producers to gain the right to export to the markets. For instance, the Office International de la Vigne et du Vin (OIV) has legislated the concentrations to 0.2 mg/L As, 0.01 mg/L Cd, 1 mg/L Cu, 0.2 mg/L Pb, 60 mg/L Na, and 5 mg/L Zn (15).

It is well-known that several elements in the finished wine influence both its stability and its color and clarity. During the wine-making process, iron may form insoluble precipitates or colloidal forms which flocculate and result in undesirable turbidity (16–17).

The origin of copper in wine can be attribued to exogenous origins or to the very nature of the grapes themselves. High concentrations of this metal can be attributed to the application of copper-based compounds (copper sulphate, dicopper chloride trihydroxide) to the grapevine as a plant fungicide. Copper is also responsible for turbidity and unfavorable flavor changes (17–18). Zinc is responsible for undesirable flavors in wine and its presence in the final product could be due to leaching from the equipment and containers or be the result of anti-fungi treatments of the grapes (17,19). Manganese affects the fermentation process and is characteristic of the production region (14,17).

Determination of the concentration of metallic elements in wine is also useful to calculate the daily intake of such elements. Several studies reveal that wine is an important source of iron (17).

On the other hand, some metal elements are to be investigated because of their toxicity and potential health effects.

Chromium is an essential element for the carbohydrate, cholesterol, and protein metabolism, while Cr toxicity depends on the metal's chemical form. Cr(VI) compounds show a toxic, mutagenic, and even carcinogenic character. Cr(III), which is the most frequently found form in foods and beverages, has low toxicity. Although humans can absorb Cr compounds by inhalation or dermal contact, Cr intake through diet is the most important route of entry into humans (20–23).

**Corresponding augthro.*
E-mail: mrivero@latu.org.uy

Cadmium is considered as toxic as lead and mercury, and its determination has gained attention as a result of its effect on health. High level Cd contamination in wine might be caused by the application of pesticides and fertilizers (24).

Health concerns regarding lead content in wines have been raised during the last decades. High levels of this metal in wine have been explained to be due to sources such as soil, lead-based insecticides (although now prohibited in most locations, it has been used as a caterpillar insecticide), and lead paint. The use of brass components such as pumps, valves, faucets, and piping also are large contributors to Pb contamination found in wine.There is some controversy concerning the uptake of Pb by vines grown in vineyards close to major highways (24–30).

Not surprisingly, the average concentration of some toxic elements, especially Pb, in wine has been decreasing worldwide due to improved wine-making techniques and equipment, and a decreased use of pesticides. But, interestingly, metals associated with stainless steel (Ni, Cr) have been rising (31–32).

Methods described for the determination of metal elements in wine include atomic absorption spectrometry (AAS) (33–36), inductively coupled plasma atomic emission spectrometry, inductively coupled plasma mass spectrometry (37), potentiometric stripping analysis, and differential pulse anodic stripping voltammetry (38).

Among these methods, the most commonly used is AAS because of its versatility, precision, and accuracy. The recommended technique for the determination of Cu, Fe, Mn and Zn in wine is flame AAS. Trace element determination is performed with a more sensitive technique such as graphite furnace atomic absorption spectrometry (GFAAS). This methodology is employed by the OIV for the quantification of lead and cadmium, and is also suggested in the literature for chromium determination (15).

EXPERIMENTAL

Instrumentation

A PerkinElmer Model 5000 atomic absorption spectrometer: (PerkinElmer Life and Analytical Sciences, Shelton, CT, USA), equipped with a deuterium arc background corrector.

For ETA-AAS determinations, the same spectrometer was used equipped with a PerkinElmer HGA®-500 graphite furnace and pyrolytically coated graphite tubes. Argon gas was used to protect and purge the graphite tubes.

The instrumental settings, furnace programs, and working conditions are listed in Tables I and II.

TABLE I
Working Conditions for the Determination of Cu, Fe, Mn, and Zn

Element	Wavelength (nm)	Slit Width (nm)	Flame Type	Light Source	Linear Working Range (mg/L)
Cu	324.8	0.7	AAOF	HCL	0.020–0.90
Fe	248.3	0.2	AAOF	HCL	0.050–4.0
Mn	279.5	0.2	AAOF	HCL	0.060–4.0
Zn	213.9	0.7	AAOF	HCL	0.010–0.25

AAOF = air-acetylene oxidizing flame; HCL = hollow cathode lamp.

Water purification was performed using a Milli-Q™ Plus purifier system (Millipore Corp., Bedford, MA, USA).

Reagents and Solutions

All reagents were of analytical grade or better.

Standard stock solutions of elements were of 1000 µg/mL Cd, Cr, Cu, Fe, Mn, Pb, and Zn (J.T. Baker, Inc., USA), certified by the manufacturer to ±1% (w/v) traceable to NIST (National Institute of Standards and Technology, Gaithersburg, MD, USA).

Nitric acid, 65% (E. Merck). Nitric acid 1% was used for wine dilution.

All solutions were prepared with deionized water with specific resistivity of 18MΩ.cm.

A 10% (w/v) Triton® X-100 (Merck) solution was made by diluting 1 g of Tritron X-100 to 10 mL with deionized water.

Matrix modifier, ammonium dihydrogen phosphate (Suprapur®, Merck, 1.01440). The matrix modifier solution was prepared by dissolving 1 g $NH_4H_2PO_4$ in 50 mL 0.3% (v/v) HNO_3. The final solution was diluted to 100 mL with 0.3% (v/v) HNO_3.

The wine matrix consisted of 100 mL absolute alcohol, 7.0 g citric acid, 3.0 g sucrose, 2.0 g glycerol, 3.8 g tartaric acid, 1.5 mL phospohoric acid, and up to 1000 mL deionized water.(39)

Recovery solution test: In order to perform recovery studies of the these elements in wine, a known amount of Cd, Cr, Cu, Fe, Mn, Pb, and Zn was added to a wine sample. The metal concentrations were made to contain 2 ng/mL Cd, 8 ng/mL Pb, 8 ng/mL Cr, 0.3 mg/L Cu, 0.08 mg/L Zn, 1 mg/L Fe, and 2 mg/L Mn (the concentration was intended to be at the center of the

TABLE II
Instrumental Conditions and Furnace Programs for the Determination of Cd, Cr and Pb

	Cd	Cr	Pb
Wavelength (nm)	228.8	357.9	283.3
Low slit setting (nm)	0.7	0.7	0.7
Light source	HCL	HCL	HCL
Drying temperature (°C)	110	110	110
Ramp (s)	5	5	5
Hold(s)	50	50	50
Flow rate (mL/min)	300	300	300
Ashing temperature (°C)	300	500	1000
Ramp (s)	5	10	15
Hold(s)	10	10	10
Flow rate (mL/min)	300	300	300
Atomization temperature (°C)	2100	2300	2700
Ramp (s)	1	1	1
Hold(s)	5	5	5
Flow rate (mL/min)	0	0	0
Cleaning temperature (°C)	2700	2700	2700
Ramp (s)	1	1	1
Hold(s)	2	2	2
Flow rate (mL/min)	300	300	300
Chemical modifier	$NH_4H_2PO_4$	$NH_4H_2PO_4$	0.5% HNO_3
Injection volume sample/modifier (µL)	20/5	20/5	20/5
Background correction	D_2 Lamp	D_2 Lamp	D_2 Lamp
Measurement mode	Peak Area/ Height	Peak Area/ Height	Peak Area/ Height

calibration curve). The sample was spiked with a certified solution, Trace Metal Standard I (J.T. Baker Inc., USA).

Procedure

To obtain extensive data for this work, 47 different brands of fine Uruguayan wines were analyzed. The samples were homogenized in the original bottles for 15 min in an ultrasonic bath prior to sampling. This was done to ensure that the precipitate in some wines was dissolved. Wine bottle tops were scrubbed and rinsed prior to cork extraction. All sample manipulations were performed using autopipettes with disposable tips.

Determination of Cd, Cr and Pb

The wine samples were diluted 1 to 4 by mixing 200 µL of wine with 800 µL of 1% HNO_3. To each diluted sample, 3 µL of a 10% solution of Triton X-100 was added. The samples were injected manually onto the wall of the graphite tube with a micropipet. The chemical modifier was injected soon after the sample and the method of standard addition was used.

Determination of Cu, Fe, Mn, and Zn

To avoid pre-treatment of wines, a calibration curve was prepared in a wine matrix simulator. Some authors reported using a matrix-matching method, which offers the ability to obtain a simple external calibration by preparing standard solutions as similar as possible to the samples (14,39,40).

The calibration curve covers the range of 20–1000 ng/mL Cu, 10–250 ng/mL Zn, 50–3000 ng/mL Fe, and 60–4000 ng/mL Mn.

RESULTS AND DISCUSSION

The results of the analysis of the wines examined are summarized in Table III and the analytical characteristics of the methodology used are shown in Table IV.

To calculate the detection limits, seven determinations were carried out in the wine matrix in accordance with the methodology suggested by EPA (41).The detection limits obtained are in good agreement with those reported previously using the same analytical technique (9,14,16,18,28).

The recovery study for the seven metals was performed by spiking three different wine samples with two different concentrations of standard solutions of each element. The recoveries obtained show very acceptable results (95.7% or higher) for the seven metals.

Iron

Mineral elements, such as iron, are natural constituents of wine and directly affect the final quality and characteristics of the wine. Iron normally appears in the grape as part of certain enzymes, but its concentration in wines can be increased by the type of soil, the maturity of the grape, climactic conditions, agrochemical residues, and especially by the processes involved in making the wine (44). Iron has the capacity to form compounds with a wide variety of substances, giving rise to turbidity or changes in color (blue or white shift). It also acts as a catalyst in the oxidation processes involved in

TABLE III
Results for the Determination of Cd, Cr, Pb, Cu, Fe, Mn, and Zn in Uruguayan Wines[a]

Grape Variety	Wine Type	Cd (mg/L)	Cr (mg/L)	Pb (mg/L)	Cu (mg/L)	Fe (mg/L)	Mn (mg/L)	Zn (mg/L)
Tannat	Red	DL	0.037	0.024	0.0552± 0.0055	2.54±0.22	n.d.	0.67±0.10
Merlot	Red	DL	0.017	DL	0.103± 0.012	2.10±0.17	n.d.	1.10±0.17
Tannat	Red	DL	0.023	0.013	0.0713± 0.0069	2.34±0.18	n.d.	0.99±0.15
Cabernet-Sauvignon	Red	DL	0.031	0.010	0.0580± 0.0050	2.87±0.19	n.d.	0.74±0.11
Merlot	Red	DL	0.052	0.023	0.140± 0.014	2.31±0.15	n.d.	0.97±0.15
Tannat	Red	DL	0.014	0.009	0.0704± 0.0067	2.15±0.43	n.d.	1.43±0.21
Merlot	Red	DL	0.013	0.018	0.149± 0.15	1.91±0.23	n.d.	0.81±0.12
Merlot	Red	DL	0.025	0.015	0.101± 0.010	4.64±0.37	n.d.	0.643± 0.096
Tannat	Red	DL	0.008	0.042	0.0604± 0.0060	2.50±0.23	1.431±0.098	0.590± 0.089
Merlot	Red	DL	0.010	0.024	0.0873± 0.0087	2.55±0.21	2.20±0.15	0.79±0.12
Cabernet-Sauvignon	Red	DL	0.009	0.006	0.0623± 0.00572	2.43±0.19	1.834± 0.13	0.566± 0.084
Cabernet-Sauvignon	Red	DL	0.038	0.057	0.331± 0.029	4.40±0.35	n.d.	0.653± 0.098
Shiraz	Red	DL	0.030	DL	0.0723± 0.0068	2.34±0.21	1.431± 0.098	0.653± 0.098
Cabernet-Sauvignon	Red	DL	0.020	DL	0.0691± 0.0073	1.35±0.11	1.50±0.13	0.624± 0.093
Merlot	Red	DL	0.027	DL	0.0860± 0.0077	1.33±0.13	1.55±0.11	0.77±0.12
Merlot	Red	DL	0.026	DL	0.0543± 0.0054	1.30±0.10	1.74±0.12	0.495± 0.074
Shiraz-Tannat	Red	DL	0.031	DL	0.103± 0.010	2.35±0.18	0.794± 0.055	0.92±0.14
Merlot	Red	DL	0.029	DL	0.0873± 0.0086	1.41±0.11	1.338± 0.091	0.78±0.12
Tannat-Merlot	Red	DL	0.030	DL	0.0580± 0.0050	1.84±0.14	2.03±0.14	0.538± 0.080
Cabernet-Sauvignon	Red	DL	0.030	DL	0.0944± 0.0089	1.74±0.14	1.233± 0.084	0.600± 0.090
Merlot	Red	n.d	n.d	n.d	0.104± 0.012	1.09±0.11	1.216± 0.085	0.125± 0.019
Tannat	Red	DL	DL	0.017	0.225± 0.021	1.84±0.14	1.44±0.12	2.00±0.030
Tannat	Red	DL	0.004	0.010	0.114± 0.014	2.13±0.17	1.44±0.14	0.95±0.14
Merlot	Red	DL	DL	DL	0.0765± 0.0073	1.43±0.11	1.53±0.11	0.68±0.10
Merlot	Red	DL	0.032	DL	0.128± 0.012	2.91±0.20	1.73±0.12	1.03±0.15
Merlot	Red	0.003	n.d.	0.020	0.0340± 0.0036	2.92±0.23	1.421± 0.099	1.14±0.24
Merlot	Red	n.d	n.d	n.d	0.192± 0.020	1.034± 0.084	1.82±0.13	0.70±0.11
Tannat-Merlot	Red	n.d	n.d	n.d	n.d	2.03±0.17	1.54±0.11	0.66±0.11
Tannat	Red	n.d	n.d	n.d	0.0713± 0.083	1.58±0.13	1.79±0.14	0.66±0.10
Merlot	Red	n.d	n.d	n.d	0.197± 0.013	1.61±0.13	1.65±0.10	0.606± 0.090
Cabernet-FrancMerlot	Red	n.d	n.d	n.d	n.d	1.247± 0.099	1.50±0.11	0.488± 0.075
Cabernet-Sauvignon	Red	n.d	n.d	n.d	0.120± 0.013	1.43±0.11	1.79±0.13	0.79±0.11
Tannat	Red	n.d	n.d	n.d	0.0746± 0.0080	1.203± 0.096	1.67±0.12	0.666± 0.099
Chardonay	White	DL	0.023	0.042	0.0890± 0.0089	1.033± 0.081	n.d.	1.43±0.21

Table III continued on next page

TABLE III (continued)
Results for the Determination of Cd, Cr, Pb, Cu, Fe, Mn, and Zn in Uruguayan Wines[a]

Grape Variety	Wine Type	Cd (mg/L)	Cr (mg/L)	Pb (mg/L)	Cu (mg/L)	Fe (mg/L)	Mn (mg/L)	Zn (mg/L)
Chardonay	White	DL	0.022	0.012	0.170±0.0017	1.30±0.11	n.d.	0.80±0.12
Chardonay	White	DL	0.020	0.030	0.0360± 0.0030	2.36±0.18	n.d.	0.594± 0.089
Sauvignon-Blanc	White	DL	0.031	DL	0.0740± 0.0065	1.34±0.14	0.943± 0.066	0.600± 0.090
Chardonay	White	DL	0.018	DL	0.230± 0.023	0.850± 0.068	1.321± 0.091	2.00±0.30
Chardonay	White	0.002	0.024	DL	n.d.	0.733± 0.058	1.65±0.11	n.d.
Chardonay-Viognier	White	n.d	n.d	n.d	n.d	2.55±0.20	1.25±0.10	2.179± 0.33
Sauvignon Gewürz-traminer	White	n.d	n.d	n.d	0.0713± 0.0069	1.155± 0.096	0.967± 0.067	0.458± 0.069
Botrytis-Noble	White	n.d	n.d	n.d	n.d	2.16±0.18	0.799± 0.055	0.631± 0.089
Chardonay	White	n.d	n.d	n.d	n.d	1.65±0.13	1.42±0.11	0.609± 0.091
Chardonay	White	DL	0.006	0.006	0.221± 0.018	0.954± 0.076	1.435± 0.078	2.00± 0.030
Sauvignon	White	n.d	n.d	n.d	0.0317± 0.0032	0.522± 0.042	1.45±0.12	0.83±0.13
Chardonay	White	n.d	n.d	n.d	0.0923± 0.011	0.144± 0.011	1.43±0.11	1.59±0.24
Chardonay	White	n.d	n.d	n.d	0.0844± 0.0076	0.493± 0.039	1.82±0.14	0.79±0.12
Typical range[b]		0.00025 - 0.0007	0.030 - 0.060	0.030 - 0.100	0.060-0.40	0.90-10.0	0.37-5.0	0.50-3.5

[a] Each value is the average of 3 replicates.

[b] Typical values of metallic ions in wines informed before (37, 43).

DL = Detection limit.

n.d.= not determined.

aging and it has an important effect on the sensorial evaluation of the product (16).

Iron levels in the samples investigated vary between 0.73 and 4.6 mg/L. These concentrations are among the lowest reported in the literature for wines (37) and indicates that no contamination occurred during the wine-making process.

Since the Fe concentration in wines does not exceed 10 mg/L, there should be no danger of ferric cloudiness and the stability of these wines should be assured (45).

Copper

Copper occurs naturally in grapes, but treatment of the vine with copper-based pesticides can result in higher concentrations of this element in wines.

This metal is found in wine at concentrations varying between 0.1 and 0.5 mg/L (46), although other authors have estimated copper levels to be closer to 1 or 3 mg/L (47). It is generally believed that the mean values taken between 0.2 and 0.4 mg/L create no problems in stability with respect to cupric cloudiness (18, 48).

The legal limit for Cu according to OIV regulations is 1 mg/L. It was found that all of the samples analyzed did not exceed 0.33 mg/L nor did they show any cupric cloudiness.

Zinc

The determination of zinc in wines has been documented extensively in the literature. Table III shows that the zinc levels in the samples analyzed were between 0.49 and 2.2 mg/L, which is well below the OIV established limit for this element in wine (5 mg/L). These values fall within the range 0.15–4.0 mg/L and are considered to be normal. The low levels found can be attributed to the specific techonological methods employed, the aging procedures of the product, and storage of the wine in

TABLE IV
Analytical Characteristics of Method to Determine Cd, Cr, Pb, Cu, Fe, Mn, and Zn

	Detection Limit (mg/L)	Recovery (%)	Precision CV (%)	Range (mg/L)
Cd	0.0005	97.8±2.5	10	0.001–0.0090
		97.9±2.5		
		99.2±2.6		
Cr	0.001	98.4±1.7	3.9	0.002-0.010
		102.7±1.7		
		103.4±1.8		
Pb	0.003	98.2±2.7	7.5	0.008-0.020
		98.7±2.7		
		100.4±2.7		
Cu	0.0055	95.9±1.3	3.6	0.020-0.090
		97.0±1.4		
		97.8±1.4		
Fe	0.021	96.5±3.1	4.0	0.050-4.0
		97.0±3.1		
		98.4±3.2		
Mn	0.0077	96.9±1.8	2.3	0.060-4.0
		97.9±1.9		
		99.5±1.9		
Zn	0.007	95.0±3.6	2.0	0.010-0.25
		95.8±3.6		
		96.3±3.7		

wooden containers. Wines kept in metallic containers usually have higher levels of zinc and other elements as well. (19)

Manganese

Manganese levels in wine are generally low. Some authors believe that they are characteristic of a specific wine-growing region, since the amount of Mn in soil is reflected in the final wine content (37). Manganese concentrations in these wines varied between 0.74 and 2.2 mg/L.

The manganese content in wines depends on the type of vinification. It is higher in red wines because during the wine-making process the must remains in contact with the solid part of the grapes for a longer period of time and dissolves the mineral salts. (49)

Chromium

Although the chromium content in wine is not regulated by the OIV, it is important to know the chromium level in wines because of its toxicity. The presence of this metal can be attributed to the use of stainless steel equipment during the wine-making process.

Chromium concentration levels were as high as 0.052 mg/L in only one sample. The other wines presented concentration levels lower than 0.034 mg/L Mn.

Taking into account that the maximum tolerance limit established by the U.S. Food and Drug Administration for drinking water is 0.100 mg/L (50), the chromium concentration found for all the samples tested in this study were far below this limit. Thus, the consumption of this fine Uruguayan wine presents no health threat.

The low concentration of this metal found in this project suggests that leaching from stainless steel is very slight.

Cadmium

From the 32 wine samples investigated, only two samples showed detectable amounts of cadmium. However, they were below the limit legislated by the OIV.

Lead

Lead content in wines deserves special consideration because of its toxicity and cumulative character (51). Health concerns regarding lead in wine have increased over the past deacade. Surveillance excercises during this period have shown that the lead content is variable (14). However, improved industrial practices in wine-making have caused a gradual reduction in lead content, which is reflected in lowering the limits set by leading organizations (52). The OIV has prescribed the limit to 0.2 mg/L Pb, with a recommendation for further reduction (15).

All the wines tested showed lower lead concentrations than the maximum limit permitted by the OIV. The highest concentration found was 0.057 mg/L for one red wine while all other wines showed concentration levels lower than 0.042 mg/L. These low lead levels found in the Uruguayan wines confirms the good production practices employed.

Further analysis of the results listed in Table III shows that there exists a correlation between wine color and metal content. Several studies indicate that element concentrations in wine are related to whether the wines were red or

white. This implies a connection with processing and/or grape variety. It is assumed that the element variability between red and white wines is reflected in the differences between grape varieties. Wines of the same color may have similar element concentrations due to processing. The grape skins contact the must during red wine fermentation which causes the extraction of anthocyanins and tannins. Higher concentrations of some metals may be related to a more efficient extraction of the elements from the skins and pulp during fermentation (9).

Iron concentrations in red wines are higher than in white wines, even for wines from the same winery. It did not seem to matter whether the wine came from the same winery or not, the iron levels appeared to be higher in red than in white wines.

In contrast, zinc concentrations in white wines are higher than in red wines. This tendency was reported before but no further explanation was given (9).

Manganese levels are frequently associated with the production region. In all of the samples for which manganese was determined, the same mean value of 1.4 mg/L was found regardless of the wine color or the winery. This may be attributed to the fact that the vineyards were located in the same area and thus the soil was of similar manganese compositon.

The reasons why the elemental composition of wines from the same winery appear to be very similar are that (a) the wines came from grapes grown on similar soil, (b) they came from the grapes of vines irrigated with water from the same source, (c) they were crushed, stored, and aged with similar equipment, or (d) they were purified and filtered by similar processes (9).

CONCLUSION

This type of project is very important since the determination of elements in wines may help protect prestigious wineries from counterfeit wines and permit source confirmation for government certification.

The methodology employed for the determination of Cd, Cr, and Pb by GFAAS, and Cu, Fe, Mn, and Zn by FAAS was appropiate and the results obtained were as expected.

Fine Uruguayan wines have received many awards and their excellence is recognized worldwide. In this work, the quality of the Uruguayan wines studied was demonstrated and confirmed with regard to their metal content. The data generated show that the cadmium, copper, lead, and zinc concentrations in the wines tested are significantly lower than the maximum tolerance limits established by the Office International de la Vigne et du Vin. Apart form this, the concentrations of all the elements determined fall within the range typical of wines from around the world.

It can also be concluded that the wines tested are stable with regard to ferric and cupric cloudiness.

ACKNOWLEDGMENTS

The author is especially grateful to Raquel Huertas for her support, guidance, and help throughout this research.

I would also like to thank to Elena Darre for her helpful review of an earlier version. I acknowledge all persons who so kindly provided helpful and pertinet comments.

I would also like to thank the staff of the Wine Department of LATU who collected and kindly donated the wine samples used for the present work.

The author also thanks the Head of the Analytical Department of the Laboratorio Tecnológico del Uruguay for his permission to use the facilities and the equipment of the laboratory to carry out this project.

Trade names are used for informational purposes only.

Received November 23, 2003.

REFERENCES

1. M. Gonzales-Larraina, A. Gonzales, and B. Medina, Connaissance de la Vigne et du Vin 21,2:127 (1987).
2. C. Herrero-Latorre and B. Medina, Journal International des Sciences de la Vigne et du Vin, 24, 4:147(1990).
3. M.J. Latorre, C. Herrero, and B. Medina, Journal International des Sciences de la Vigne et du Vin, 26, 185(1992).
4. M.P. Day, B.L. Zhang, and G.J. Martin, American Journal of Enology and Viticulture, 45, 1:79 (1994).
5. M.P. Day, B.L. Zhang, and G.J. Martin, C. Asselin, and R. Morlat, Journal International des Sciences de la Vigne et du Vin, 29, 2:75(1995a).
6. M.P. Day, B.L. Zhang, and G.J. Martin, Journal of Science and Food Agriculture, 67, 113 (1995).
7. J. B. Fournier and O. Hirsch, Actes Symp. In Vino Analytica Scientia, 532 (1997).
8. M.J. Baxter, H.M. Crews, M.J. Dennis, I. Goodall, and D. Anderson, Food Chemistry, 60, 3:443 (1997).
9. J.D. Greenough, H.P. Longerich, S.E. Jackson, Australian Journal of Grape and Wine Research, 3:75 (1997).
10. L.A. Rizzon, A. Miele, and J.P. Rosier, Journal International des Sciences de la Vigne et du Vin, 31, 1:43 (1997).
11. G. Thiel, and K. Danzer, Fresenius' J. Anal. Chem. 357, 5:553 (1997).

12. N. Jakubowski, R. Brandt, D. Stuewer, H.R. Eschnauer, and S. Gortges, Fresenius' J. Anal. Chem. 364, 5:424(1999).

13. G.J. Martin, M. Mazure, C. Jouitteau, Y.L. Martin, l. Aguile, and P. Allain, Journal International des Sciences de la Vigne et du Vin, 50, 4:409 (1999).

14. M.J. Gonzalez, M.C. Martínez Para, and M.V. Aguilar, Z Lebensm Unters. Forsch. 187:325 (1988).

15. European Union, 1990, Commission Regulation No. 267690 of 17 September 19990. Official Journal L272, 1-192.

16. M. Olalla, M.C. Gonzalez, C. Cabrera, and M.C. López, Journal of AOAC International 83:189(2000).

17. M. López-Artíguez, A.M. Cameán, and M. Repetto, Journal of AOAC International 16, 79:1191(1996).

18. A.A. Almeida, M. I. Cardoso, J.L.F.C. Lima, At. Spectrosc. March/April :75 (1994).

19. M.E. Soares, M.L. Bastos, and M.A. Ferreira, At. Spectrosc. 15, 256(1995).

20. S.M. Brichard, J. Saavedra, J. Kolanowski, and J.C. Henquin, Mëd. Hig. 51:2814 (1993).

21. M. Shils, J. Olson, and M. Shike. Modern Nutrition in the Health and Disease, Lea&Febiger, Malvern, PA (1994).

22. D. Littlefield, J. Am. Diet. Assoc. 94:1368 (1994).

23. O.R. Fennema, Food Chemistry, Marcel Dekker, New York, NY (1993).

24. R. Tahvonen, Food Additives and Contaminants 15:446 (1998).

25. A. Kaufman, Food Additives and Contaminants 15:437 (1998)

26. L. Jorhem and B. Sundström, At. Spectrosc. Sep/Oct :226 (1995).

27. M.R. Matthews, and P.J. Parsons, At. Spectrosc. 14 :41(1993).

28. W.R. Mindak, Journal of AOAC International 16, 77:1023 (1994)

29. R.G. Wuilloud, A.H. González, E.J. Marchevsky, R.A. Olsina, and L.D. Martínez, Journal of AOAC International 16, 84:1555 (2001).

30. M. Aceto, O. Abollino, M.C. Bruzzoniti, E. Mentasti, C. Sarzanini, and M. Malandrino,Food Additives and Contaminants 19:126 (2002).

31. C.S. Stockey, T.H. Lee, Journal of Wine Research 6: 5-17 (1995).

32. H. Eschnauer, American Journal of Enology and Viticulture 33:226-230 (1982).

33. C.S. Ough, E.A. Crowell, J. Benz, J. Food Sci . 47:825 (1982).

34. M.S. Larrechi, M.P. Callao, F.X. Rius, J. Guasch, Rev Agroquim. Technol. Aliment. 27:53 (1987).

35. M. Olalla, M.C. López, H, López, M. Villalón, Alimentaria 243:79 (1993).

36. M. Larroque, J.C. Cabanis, L. Viau, Journal of AOAC International 16, 77:463 (1994).

37. F.S. Interesse, F. Lamparelli, V. Alloggio, Z. Lebensm. Unters. Forsch. 178:272 (1984).

38. M. Oehme, W. Lund, Fresenius' J. Anal. Chem. 294:391 (1979).

39. M. López-Artíguez, A.M. Cameán, M. Repetto, Journal of AOAC International 79:1191 (1996).

40. M. Aceto, O. Abollino, M.C. Bruzzoniti, E. Mesntasti, C. Sarzanini, and M. Malandrino. Food Additivies and Contaminants 19:126 (2002).

41. Method of Chemical Analysis. Definition and Procedure for the Determination of the Methods Detection Limit. Appendix B to Part 136, Revision 1.11, US EPA, EMSL, Cincinati, OH, USA (1992).

42. EURACHEM/CITAC Guide. Quantifying Uncertainty in Analytical Measurement. 2nd Edition, SLR Ellison, M. Rosslein, A. Williams. (2000).

43. H. Eschnauer, L. Jakob, H. Meierer, and R. Neeb, Mikrochim. Acta 3:291 (1989).

44. P. Fernandez, Z. Lebensm. Unters. Forsch. 186:295 (1988).

45. A. Torazzo, L. Cere, F. Parcivale, A. Marcchese, Rass Chim. 34:205 (1982)

46. A. Larrea Redondo, Enología Básica. Aedos, Barcelone(1983).

47. R. Ordoñez, G. Paneque, M. Medina, L. Corral, An Edafol Agrobiol. 42:1133 (1981).

48. V. Coppola, Vignevini 9:19 (1982).

49. J. Ribéreau-Gayon, E. Peynaud, P. Sudraud, P. Ribéreau-Gayon, Tratado de Enología. Ciencias y Técnicas del Vino, vol I. Análisis y Control de Vinos. Hemisferio Sur, Buenos Aires (1980).

50. U.S. Food and Drug Administration, Vol. 21, Code of Federal Register, Chap.1 (2003).

51. G. Cerutti, S. Mannino, A. Vecchio, Riv Vitic Enol. 34:145 (1981).

52. P.A. Brereton, P. Ross, C.M. Sargent, H.M. Crews, and R. Wood, Journal of AOAC International, 80:1287 (1997)

Determination of Trace Elements in Human Milk, Cow's Milk, and Baby Foods by Flame AAS Using Wet Ashing and Microwave Oven Sample Digestion Procedures

***Mehmet Yaman and Nurhan Çokol**
Firat University, Science and Arts Faculty,
Department of Chemistry, Elazig, Turkey

ABSTRACT

Three sample digestion procedures using dry and wet ashing and microwave oven are compared for the flame atomic absorption spectrometry analysis of human milk, cow's milk, and baby food samples. Copper, Mn, Zn, and Fe were determined in the digestion solutions. Various acid mixtures were examined in conventional wet digestion using a hot plate. It was found that the mixture of HNO_3/H_2O_2 (1:1) was simple to use and provided best results in comparison to either $HNO_3/HClO_4$ or HNO_3 in wet ashing procedure.

The analytical parameters show that the microwave oven digestion procedure provided best results as compared to the wet ashing procedure. Microwave sample digestion is an accurate, simple, and fast method for the flame AAS determination of Cu, Mn, Zn, and Fe in human milk, cow's milk, and baby formulas, except for the determination of Fe in rice flour and baby biscuits.

INTRODUCTION

Human milk, under non-pathological states, is a well-balanced food that provides the infant with the essential elements. The element concentration ranges in human milk are generally used as a reference in manufacturing infant formulas (1). In addition, studies on the total content of the essential elements in human milk are useful to evaluate the ideal food for the first months of an infant's life.

While Cu and Zn are essential elements for infant development, they can also become toxic when taken in excess. Toxicity or the amount of an element required to maintain an infant's health varies from element to element. Milner (2) reported that the concentrations of Zn, Mn, Fe, and Cu are higher in infant formulas than in human milk, while cow's milk has a lower Cu content. Thus, infants who are provided a strictly cow's milk diet may develop Cu deficiency and anemia. Farida et al. (3) reported that Zn intake from breast milk is inadequate during the weaning period, especially when weaning foods are introduced at an early stage. A study by Perrone et al. (4) shows that infants are at risk of developing iron deficiency if weaning foods are introduced before the infant reaches one year of age.

In ashing procedures, sample digestion is often the most time-consuming step and involves potential problems such as incomplete dissolution, precipitation of insoluble analytes, contamination, and loss of some volatile elements. In order to prevent loss of elements, closed digestion bombs are used. However, this procedure requires a prolonged time for complete dissolution.

In recent times, both commercial domestic microwave ovens (5) and commercial microwave ovens equipped with temperature and pressure regulators have become widely used because sample dissolution is faster and prevents analyte loss as well as sample contamination (6–7). On the other hand, commercial microwave ovens equipped with temperature and pressure regulators are very expensive. Therefore, an examination of using a domestic microwave oven for this purpose is very important.

In our laboratory, a flame atomic absorption spectrometry (FAAS) method was used for the determination of trace metals in foods consisting of different matrices (8–11). Although considerable information is available with regard to trace element concentrations in milk and baby foods (12–13), an accurate, reliable, and fast method for the determination of these elements is needed for diagnostic purposes.

In this study, Zn, Cu, Mn, and Fe were determined in human milk, cow's milk, and baby foods such as ready-powdered baby formula, baby biscuits (commercially available), and rice flour (home-made) using the classic wet ashing or the domestic microwave oven method as the sample digestion methods. The digestion solutions were then analyzed by flame atomic absorption spectrometry.

Corresponding author.
E-mail: myaman@firat.edu.tr

EXPERIMENTAL

Instrumentation

A Model ATI UNICAM 929 (UNICAM, England) flame atomic absorption spectrometer, equipped with ATI UNICAM hollow cathode lamps, was used for the sample analysis. The optimum instrumental conditions are given in the Table I. Slotted Tube Atom Trap (STAT) was used for improving the sensitivity of Cu by FAAS. A domestic microwave oven (Kenwood, UK) and specially made Teflon® bombs were used for the digestion procedure.

Reagents and Standard Solutions

The metal stock solutions (1000 mg L^{-1}) were prepared from their nitrate salts (Merck, Darmstadt, Germany). Nitric acid (65%, Merck), hydrogen peroxide (35%, Merck), and perchloric acid (70%, Merck) were used for the sample digestions.

Digestion of Samples by Wet Ashing

Human milk samples were provided by Firat University and the local state hospitals. The cow's milk samples were collected in precleaned polyethylene bottles. Approximately 10 mL of cow's milk was accurately measured into Pyrex® vessels, 5 mL of HNO_3/H_2O_2 (1:1) was added; the mixture was then dried on a hot plate with occasional stirring. The same procedure was repeated using 2.5 mL of HNO_3/H_2O_2 (1:1). Then, 2.0 mL of 1.0 mol L^{-1} HNO_3 was added to the residue and centrifuged to obtain a clear solution.

The same procedures and volumes were applied to the new 10-mL sample of the same cow's milk by using HNO_3 instead of HNO_3/H_2O_2 (1:1).

A 0.75-g sample of ready-made powdered infant formula (Humana 3) was accurately weighed into Pyrex vessels, 3.0 mL of concentrated HNO_3/H_2O_2 (1:1) was added, and the mixture was dried on a hot plate with occasional stirring. The same procedure was repeated using 1.5 mL of HNO_3/H_2O_2 (1:1). Then, 2.0 mL of 1.0 mol L^{-1} HNO_3 was added to the residue and centrifuged to obtain a clear solution.

The same procedures and the same volumes described above for infant formula were also applied to the new 0.75-g sample of the same infant formula (Humana 3) by using HNO_3 instead of HNO_3/H_2O_2 (1:1).

In addition, the mixture of $HNO_3/HClO_4$ (1:1) was used as the digesting reagent instead of HNO_3/H_2O_2 for the new sample of the same infant formula, using the same procedures and volumes described above. Then, 3.0 mL and 1.5 mL of $HNO_3/HClO_4$ (1:1) were added to 0.75 g of the same infant formula in the first and second step described above, respectively. The blank digests were carried out in the same way.

Digestion of Samples by Microwave Oven

Different baby foods such as the ready-made powdered infant formula, rice flour (home-made), and baby biscuits (commercial) were digested by using a microwave oven as follows: Approximately 0.5 g of the sample was accurately weighed into Pyrex vessels. Then, 2.0 mL of concentrated HNO_3/H_2O_2 (1:1) was added and the mixture placed into a water bath at 70°C for 60 min with occasional stirring. After adding 2.0 mL of HNO_3/H_2O_2 (1:1) diluted with water (1:1), the mixture was transferred into a Teflon bomb. The bomb was closed, placed inside the microwave oven, and microwave radiation was carried out for 4 min. After a 4-min cooling period, the mixture was dried on a hot plate. Then, 2.0 mL of 1.0 mol L^{-1} HNO_3 was added and the mixture transferred to a Pyrex tube.

In addition, 5.0 mL each of cow's milk and human milk were accurately measured into Pyrex vessels, separately. Then, 2.5 mL of concentrated HNO_3/H_2O_2 (1:1) was added to the milk sample. The mixture was placed into a water bath at 70°C for 60 min with occasional stirring. After adding 2.0 mL of HNO_3/H_2O_2 (1:1), the mixture was transferred into a Teflon bomb. The bomb was closed, placed inside the microwave oven, and microwave radiation was carried out for 4 min. After a 4-min cooling period, the mixture was dried on a hot plate. Then, 1.5 mL of 1.0 mol L^{-1} HNO_3 was added and the mixture transferred to the Pyrex tube.

After centrifugation, the clear solutions were analyzed by FAAS. Blank digests were carried out using the same procedures.

TABLE I
Instrumental Operating Parameters for FAAS

Parameter	Cu	Mn	Zn	Fe
Wavelength (nm)	324.8	279.5	213.9	248.3
HCL Current (mA)	4.5	11.5	9.5	15
Acetylene Flow Rate (L/min)	0.5	0.5	0.5	0.5
Air Flow Rate (L/min)	4.0	4.0	4.0	4.0
Slit (nm)	0.5	0.2	0.5	0.2

RESULTS AND DISCUSSION

Calibration curves were obtained using Cu solutions of 0.025, 0.05, 0.1, 0.2, 0.4, and 0.8 mg L^{-1}; Mn and Zn solutions of 0.1, 0.2, 0.4, 0.8, and 1.0 mg L^{-1}; and Fe solutions of 0.25, 0.5, 1.0, 2.0, and 3.0 mg L^{-1}. The curves obtained were linear in the concentration range described above and the equations of the curves were as follows:

Copper

$Y = 205 X + 7$
$R^2 = 0.9994$
using STAT-FAAS

Manganese

$Y = 136.8 X + 4.8$
$R^2 = 0.9997$

Zinc

$Y = 327 X + 6.6$
$R^2 = 0.9998$

Iron

$Y = 69.8 X + 0.4$
$R^2 = 1.0$

Accuracy

The accuracy of the method was studied by examining the Standard Reference Material (Tomato Leaves-1573a). The results are given in Table II. It can be seen that the recovery values were 100% for Cu, 94% for Zn, 90% for Mn, and 80% for Fe. In addition, the accuracy of the method was studied by examining the recovery of the metals from cow's milk and baby formula samples fortified with different amounts of Cu, Mn, Zn, and Fe. The following metal amounts were added:
20 ng/mL of Cu and Mn, 200 ng/mL of Fe and 2000 ng/mL of Zn for cow's milk; and
500 ng/g of Cu and Mn, 30 000 ng/g of Fe and Zn for ready-made powdered baby formula (Humana 3).
After digestion by microwave oven, the recoveries were found to be at least 95% for all metals.

The standard additions method was used to investigate possible interferences caused by the matrix. The slopes of the calibration curves for all studied elements were compared with the slopes obtained by the standard additions method. The slopes of the calibration curves were found to be the same as those

TABLE II
Comparison of Digestion Methods for Reference Material, Cow's Milk, and Baby Formula and the Effect of Acid Mixtures Using Wet Digestion (n=5)

Sample		(Watt)	Cu	Mn	Zn	Fe
Cow's milk (ng/mL)						
	HNO_3		55±4	18±1.4	2650±210	375±25
	HNO_3/H_2O_2		60±5	20±1.6	2800±205	350±26
Our domestic microwave oven		360 W	61±5	18±1.6	2750±225	390±30
		450 W	45±4	20±1.5	2900±230	381±28
Ready-made powdered baby formula, Humana 3 (mg/kg)						
Wet ashing	HNO_3		5.2±0.4	0.33±0.02	44±4	51±4
	HNO_3/H_2O_2		5.0±0.4	0.36±0.03	50±5	63±5
	$HNO_3/HClO_4$		4.5±0.4	0.35±0.02	48±4	61±5
Dry ashing	Humana 3		5.0±0.3	0.30±0.02	45±4	59±5
	SMA		3.5±0.2	1.1±0.07	31±2	64±5
ETHOS plus MILESTONE microwave oven	Humana 3		4.5±0.4	0.36±0.02	45±4	65±6
	SMA		3.4±0.2	1.1±0.1	32±3	69±6
Our domestic microwave oven						
	Humana 3	360 W	5.0±0.4	0.36±0.02	50±4	63±5
		450 W	4.9±0.4	0.40±0.03	47±4	61±6
	SMA	360 W	3.5±0.2	1.2±0.08	32±2	68±5
		450 W	3.2±0.2	1.0±0.07	30±2	67±6
Reference material (Tomato Leaves 1573a)						
Certified value (mg kg^{-1})			4.7±0.14	246±8	30.9±0.7	368±7
Our domestic microwave oven		360 W	4.7±0.4	211±15	28±2	280±19
		450 W	4.7±0.4	221±17	29±2	295±21

obtained with the standard additions method. In other words, all standard additions curves were parallel to the calibration curves; the results indicate an absence of chemical interferences. Thus, calibration with aqueous standards was valid.

The possibility of sample contamination was studied by subtracting the values obtained for the blanks. Adsorption loss can be excluded as the procedure was followed in exactly the same way as described above, using the same glassware and the same reagents throughout. The results showed that there was no contamination or adsorption loss.

On the other hand, Standard Reference Material Tomato Leaves 1573a, powdered baby formulas (Humana 3 and SMA), and cow's milk were digested by using a microwave oven at the different powers of 360 and 450 W. As can be seen from Table II, significantly higher Cu levels were obtained by using 360 W for cow's milk. For other matrices, the obtained concentrations of all elements at 360 W were generally higher or close to the concentrations at 450 W using the microwave oven.

The baby formulas (Humana 3 and SMA) were also digested using a commercial microwave oven equipped with temperature and pressure regulators (MILESTONE ETHOS Plus with MPR-300/125 medium pressure rotor). The obtained results were found to be very close to the results obtained with the domestic microwave oven (Table II).

The analytical parameters obtained in the recovery assays using microwave oven digestion of cow's milk and human milk and the powdered baby's formula samples showed that the method is simple and fast for the determination of Cu, Mn, Zn, and Fe. However, the Fe determination in rice flour and baby biscuits was not good. This is attributed to the fact that the rice flour and baby biscuit samples were not sufficiently digested by the microwave oven method for Fe determination.

Comparison of Acid Mixtures With Ashing Methods

The determination of Cu, Mn, Zn, and Fe in cow's milk and powdered baby formula (Humana 3) using different acid mixtures in the wet ashing method are given in Table II. It can be seen that the analyte concentrations of the baby formula when using HNO_3/H_2O_2 (1:1) is higher in comparison to using either $HNO_3/HClO_4$ (1:1) or HNO_3. For cow's milk, the analyte concentration when using HNO_3/H_2O_2 (1:1) is slightly higher in comparison to using HNO_3, except for the Fe concentration. Iron concentrations in the HNO_3/H_2O_2 (1:1) digestions are slightly lower than in HNO_3 digestions. Therefore, HNO_3 had to be used as the wet digestion reagent for iron determination in milk samples.

In addition, the powdered baby formulas (Humana 3 and SMA) were digested by dry ashing at 480°C for 4 h and the results are given in Table II. It was found that the examined metal levels in both baby formulas were lower or equal to the levels of the microwave or wet ashing methods.

Table III shows that the Cu concentrations in all examined samples using the closed-vessel microwave oven method are very close to the Cu concentrations in the classic wet ashing method (at least 95% recovery). Particularly in the rice flour samples, slightly higher Cu levels were obtained when the microwave oven was used. For Mn concentrations, the evaluations described above for Cu were valid.

Table IV shows that the Zn concentrations in the samples using closed-vessel microwave oven were very close to the Zn concentrations obtained in the classic wet ashing method, except for the infant formulas (87% recovery).

In comparing the wet ashing and microwave methods, it was found that for the rice flour and baby biscuit samples, higher Zn levels were obtained with the microwave oven (Table IV). Although the Zn concentrations obtained for the baby formulas using wet ashing were slightly higher than the Zn concentrations obtained using microwave oven, these differences were not significant. For Fe concentrations, acceptable recoveries were obtained (90% recovery) using microwave oven in comparison to wet ashing, except for the rice flour and the baby biscuit samples.

Metal Concentrations in Baby Foods With Different Matrices

The concentration ranges of the elements considered in human milk and cow's milk were within the ranges reported in the literature (13). The values in Tables III and IV were obtained by using HNO_3/H_2O_2 (1:1) for wet ashing and 360 W for microwave oven. The observed metal concentrations using microwave oven can be summarized as follows.

The Cu content of the samples (Table III) ranged from 19–21 ng mL^{-1} for cow's milk, 200–300 ng mL^{-1} for human milk, and 0.8–3.6 mg kg^{-1} for the powdered baby formulas. The Cu content in the examined cow's milk was at the lower end of the range as reported in the literature. It can be seen that the Cu content in the human milk samples was approximately 10-fold higher than in cow's milk. However, even this concentration level would make the daily intake much lower than the recommended value of 0.5–1.0 mg/day due to an average production of 700 mL of human milk

TABLE III
Comparison of Cu and Mn Concentrations in Baby Foods Using Wet Ashing (HNO_3/H_2O_2 (1:1)) and Microwave Oven (at 360 W) [human milk (n= 3); for other samples (n= 5)]

Samples	Cu		Mn	
	Wet Ashing	Microwave	Wet Ashing	Microwave
Cow's milk 1 (ng/mL)	23±1.7	21±1.5	20±1.6	21±1.6
Cow's milk 2 (ng/mL)	22±1.6	21±1.6	21±1.7	20±1.5
Cow's milk 3 (ng/mL)	20±1.5	19±1.5	20±1.5	19±1.5
Cow's milk 4 (ng/mL)	20±1.5	20±1.5	22±1.5	23±1.6
Cow's milk 5, ng/ml	25±1.6	20±1.5	19±1.6	20±1.5
Cow's milk 6, ng/ml	60±5.0	61±4	20±1.6	18±1.5
Human milk 1(ng/mL)l (11 days*)	290±15	275±15	14±1.3	14±1.3
Human milk 2 (ng/mL) (12 days*)	325±17	300±16	15±1.2	15±1.2
Human milk 3 (ng/mL) (24 days*)	265±15	240±15	14±1.2	14±1.2
Human milk 4 (ng/mL) (24 days*)	280±14	260±14	15±1.3	14±1.2
Human milk 5 (ng/mL) (41 days*)	230±16	200±15	13±1.2	13±1.1
Baby foods:				
Rice flour (mg/kg)	0.98±0.06	1.1±0.06	8.7±0.5	10.5±0.6
Baby biscuit (mg/kg)	0.53±0.04	0.51±0.03	4.1±0.2	3.9±0.2
Powdered baby formula, SMA (mg/kg)	3.6±0.11	3.5±0.2	1.0±0.1	1.2±0.08
Powdered baby formula, Humana 3 (mg/kg)	5.0±0.3	5.0±0.3	0.36±0.02	0.36±0.02
Powdered baby formula, Guigoz (mg/kg)	3.7±0.19	3.6±0.21	0.3±0.03	0.29±0.03

*The number of days for human milk represents the days since the birth of the infant when the milk was sampled.

TABLE IV
Comparison of Zn and Fe Concentrations in Baby Foods Using Wet Ashing (HNO_3/H_2O_2 (1:1)) and Microwave Oven (at 360 W) [human milk (n= 3); other samples (n= 5)]

Samples	Zn		Fe	
	Wet Ashing	Microwave	Wet Ashing	Microwave
Cow's milk 1 (mg/L)	2.8±0.13	2.7±0.13	0.19±0.02	0.17±0.02
Cow's milk 2 (mg/L)	2.9±0.13	2.8±0.12	0.22±0.02	0.18±0.02
Cow's milk 3 (mg/L)	2.8±0.13	2.8±0.13	0.20±0.02	0.17±0.02
Cow's milk 4 (mg/L)	3.0±0.16	2.9±0.13	0.18±0.02	0.16±0.02
Cow's milk 5 (mg/L)	2.7±0.17	2.6±0.12	0.21±0.02	0.18±0.02
Cow's milk 6 (mg/L)	2.8±0.19	2.8±0.15	0.35±0.02	0.39±0.03
Human milk 1 (mg/L) (11 days*)	3.3±0.018	3.1±0.13	0.52±0.03	0.46±0.03
Human milk 2 (mg/L) (12 days*)	3.5±0.20	3.3±0.22	0.52±0.03	0.45±0.03
Human milk 3 (mg/L) (24 days*)	1.8±0.014	1.6±0.11	0.60±0.03	0.56±0.03
Human milk 4 (mg/L) (24 days*)	1.5±0.01	1.3±0.09	0.72±0.04	0.66±0.04
Human milk 5 (mg/L) (41 days*)	1.5±0.01	1.3±0.10	0.58±0.03	0.51±0.03
Baby foods:				
Rice flour (mg/kg)	9.4±0.5	9.8±0.5	4.2±0.3	3.4±0.2
Baby biscuit (mg/kg)	4.1±0.3	4.5±0.3	5.0±0.3	3.3±0.2
Powdered baby formula, SMA(mg/kg)	33±3	32±2	69±6	68±5
Powdered baby formula, Humana 3 (mg/kg)	50±4	50±3	63±5	63±4
Powdered baby formula, Guigoz (mg/kg)	39±2	37±2	59±3	55±3

*The number of days for human milk represents the days since the birth of the infant when the milk was sampled.

within 24 h during the first year of lactation (14).

The Mn concentrations of the examined samples (Table III) ranged from 19–23 ng mL^{-1} for cow's milk, 13–15 ng mL^{-1} for human milk and 0.20–1.05 mg kg^{-1} for powdered baby formulas. As reported in the literature (15), the Mn levels in human milk were lower than in cow's milk.

The Fe content of the examined samples (Table IV) ranged from 0.16–0.18 mg L^{-1} for cow's milk, 0.45-0.66 mg L^{-1} for human milk, and 54-55 mg kg^{-1} for the powdered baby formulas. The cow's milk contained a low Fe concentration, similar to Cu. In addition, it is reported that the fractional absorptions of Fe, Zn, and Mn are better from human milk than from cow's milk. Based on these facts, infants provided solely with a diet of cow's milk may become Fe deficient and develop anemia.

The Zn content of the samples (Table IV) ranged from 2.6–2.9 mg L^{-1} for cow's milk, 1.3–3.1 mg L^{-1} for human milk, and 26–37 mg kg^{-1} for the powdered baby formulas.

CONCLUSION

This study shows that closed-vessel microwave digestion of the samples and determination of the elements by FAAS is accurate, rapid, and simple. The analytical parameters obtained make this method suitable for the determination of Cu, Mn, Zn, and Fe in human milk and cow's milk and various baby foods. We found that there are no safety concerns when using a domestic microwave oven at the studied conditions because of the predigestion of the sample in a water bath for 1 h and using the Teflon bomb (durable to 360°C).

Received December 17, 2002.
Revision received June 21, 2004.

REFERENCES

1. B. Bocca, A. Alimati, E. Coni, M. Di Pascuale, L. Giglio, A.P. Bocca and S. Caroli, Talanta 53, 295 (2000).
2. J.A. Milner, J. Pediatrics 117(2), 147 (1990).
3. M.A. Farida and T.S. Srikumar, Nutrition 16, 1069 (2000).
4. L. Perrone, L. Di Palma, R. Di Toro, G. Gialanella and R. Moro, Biological Trace Element Research 41, 321 (1994).
5. R.A. Nadkarni, Anal. Chem. 56, 2233 (1984).
6. F.E. Smith and E.A. Arsena, Talanta 43, 1207 (1996).
7. M.D. Silvestre, M.J. Lagarda, R. Farre, C. Martinez-Costa and J. Barnes, Food Chemistry 68, 95 (2000).
8. S. Gucer and M. Yaman, J. Anal. At. Spectrom. 7(2),179 (1992).
9. M. Yaman, Mikrochim. Acta 129(1-2), 115 (1998).
10. M. Yaman, Commun. Soil Sci. Plant Anal. 31(19–20), 3205 (2000).
11. M. Yaman, J. Anal. Chem. 56(5), 417 (2001).
12. J.G. Dorea, Nutrition 16, 209 (2000).
13. W. Mertz, Trace elements in human and animal nutrition, Vol. 1-2, Academic Press, San Diego, CA, USA (1987).
14. R.M. Tripathi, R. Raghunath, V.N. Sastry and T.M. Krishnamoorthy, Sci. Total Environ. 227, 229 (1999).
15. C. Ekmekcioglu, Nahrung 44(6), 390 (2000).

Rapid Determination of Chemical Oxygen Demand by Flame AAS Based on Flow Injection On-line Ultrasound-assisted Digestion and Manganese Speciation Separation

***Zhi-Qi Zhang[a,b], Hong-Tao Yan[b], and Lin Yue[a]**

[a] School of Chemistry and Materials Science, Shaanxi Normal University, Xi'an 710062, P.R. China

[b] Department of Chemistry, Northwest University, Xi'an 710069, P.R. China

ABSTRACT

A rapid flame atomic absorption spectrometry (FAAS) method for the determination of chemical oxygen demand (COD) is proposed. It is based on using ultrasonic wave to advance sample digestion by potassium permanganate and flow injection on-line speciation separation of manganese. In a digestion coil, placed in the ultrasonic and heating water bath, the sample was oxidized by acidic potassium permanganate to produce Mn^{2+}. Passing through a cooling coil, Mn^{2+} was adsorbed on a cation-exchange micro-column, while the unreduced MnO_4^- passed through the micro-column to waste. Then the adsorbed Mn^{2+} was eluted reversely by 3 mol L^{-1} HCl and determined by FAAS. With a digestion temperature of 80˚C and a digestion time of 30 s, the determination range was 3-300 mg L^{-1} COD and the detection limit was 1 mg L^{-1} COD, with a sampling frequency of 24 samples per hour. The relative standard deviation of the method was 2.7 % (n=9). Chloride did not interfere up to the 1000-mg L^{-1} level. The proposed method was applied to the determination of COD in well, river, and pool water samples, and the results obtained are in agreement with those given by the standard methods.

INTRODUCTION

Chemical oxygen demand (COD) refers to the amount of oxygen necessary for the oxidation of all organic matter contained in a water sample; it is a widely used parameter in controlling the degree of pollution in water and managing effluent quality. The conventional and standard method for COD determination consists of two steps: (a) oxidizing digestion by adding a strong oxidant such as potassium permanganate or potassium dichromate to the given samples of water and refluxing at high temperature, and (b) titration of excess oxidant (1,2). This methodology is manual and suffers from a series of drawbacks such as being very time-consuming (two hours are required for digestion plus time for titration) and requiring a high amount of expensive (Ag_2SO_4) and toxic ($HgSO_4$) chemicals. Much effort has been devoted to the improvement and alteration of the standard manual method, and many research results have been reported (3–20).

Flow injection analysis (FIA) is becoming one of the most important tools for routine work because it is a simple and inexpensive method with high analysis speed, high precision, and suitable for on-line analysis. These advantages make FIA especially interesting for routine COD determinations. Korenaga and co-workers made the first attempts in this respect and reported the possibility of determining COD using the FIA techniques with potassium permanganate (3,4), potassium dichromate (5), and with Ce(IV) (6) as the oxidant. Further studies were done by Appleton (7), Balconi (8), and Pecharroman (9). Segmented flow analysis (SFA) to COD determination was applied by Tian (10).

All of the above-mentioned flow systems show higher analysis speed than the conventional method. However, the big difference in time required for heating digestions between the conventional method (2 h) and flow methods (a few minutes) means that in some cases there is a difference in the degrees of sample oxidation, with the possibility of a difference in COD values obtained. In order to enhance the efficiency of digestion, microwave radiation (MW) has been applied to the digestion step in a FIA system for COD determination (11–14). It is well known that ultrasonic waves can quicken chemical reaction and enhance productivity (21). In recent years, ultrasonic waves have been widely used in the destruction of organic pollutants (22,23) and oxidization digestion (24). Aiguo Zhong (15) recently presented a method for COD determination based on the use of ultrasonic digestion, but not with a FIA system.

Spectrophotometry is the most common detector used for COD determination by FIA, but this non-specific detector has some drawbacks. Signals are frequently unstable due to bubble formation, which imposes an upper limit to the applied temperature in the digestion step and causes a decrease in the degree of complete oxidation of the organic matter in the water sample. Flame atomic absorption spectrometry (FAAS) is superior in terms of speed, sensitivity, and selectivity, and is very suitable for metal determination in liquid samples. However, its application to COD determination is

**Corresponding author.*
E-mail: zqzhang@snnu.edu.cn

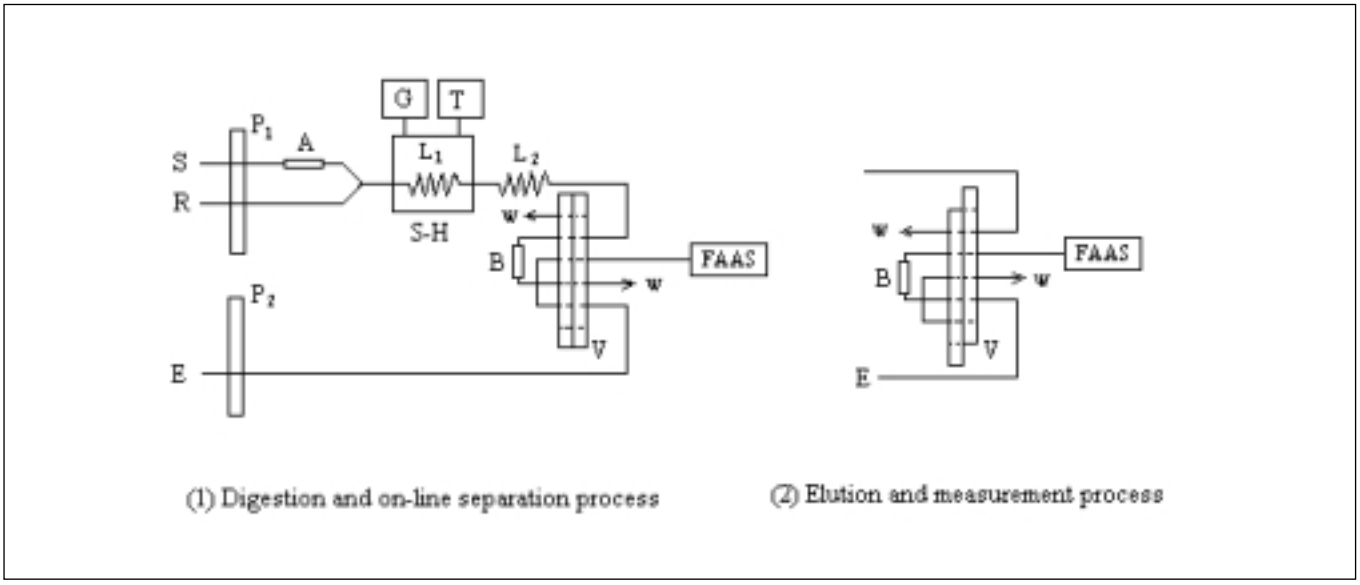

Fig. 1. Schematic of the ultrasound-assisted digestion/flow injection on-line separation system for the determination of COD. S = sample; R = acidic $KMnO_4$ solution; E = water or HCl solution; P_1 and P_2 = peristaltic pumps; L_1 = digestion reaction coil (about 1 mm i.d. and 500 cm in length, made of glass); L_2 = cooling coils (1 mm i.d. and 50 cm in length); S-H = ultrasonic and heating water bath; G = ultrasonic generator; T = thermostat; V = injection valve; A and B = cation exchange micro-columns (2 mm i.d. and 50 mm in length); FAAS = flame atomic absorption spectrometer; W = waste.

hampered by the need of a separation step for different species of the same element such as Cr(VI) and Cr(III), Mn(VII) and Mn^{2+}. Cuesta et al. (13) presented a FI-FAAS for COD determination in which MW heating digestion of the sample with potassium dichromate was followed by ion exchange (13) or extraction (14), and separation of Cr(VI) from Cr (III). Recently, Lee et al. (16) proposed an electrochemical COD sensor and Kim et al. (17,18) proposed a photocatalytic sensor based on using an oxygen electrode for COD determination.

In this paper, a rapid ultrasonic digestion with a cation exchange column on-line separation of Mn^{2+} from Mn(VII) is proposed using a FI-FAAS system for COD determination. Satisfactory results were obtained in the determination of COD in well, pool, and river water samples.

EXPERIMENTAL

Instrumentation

A Model TAS-986 atomic absorption spectrometer (Beijing Purkinje General Instrument Corporation, P.R. China), equipped with a hollow cathode manganese lamp, was used to measure the absorbance of Mn^{2+}. The wavelength and lamp current used were 279.5 nm and 2.0 mA, respectively. About 1700 mL min^{-1} of acetylene and 8000 mL min^{-1} of air flow were employed to obtain a steady flame. A computer was used to record the absorbance peaks.

A Model IFIS-C intellectual flow injector (Xi'an Ruike Electron Equipment Corporation, P.R. China) was used to design the FI system.

A Model ACQ-600 ultrasonic generator (Shaanxi Xiangda Ultrasonic Technology Engineering Department, P.R. China) and a Model 501 thermostat (Shanghai Experimental Apparatus Factory, P.R. China) were employed to provide ultrasound-assisted and heating digestion conditions.

Design of Flow Injection System

The flow injection system used in this work was similar to the one used for the indirect determination of ciprofloxacin (25), but the reaction coil (L1) was placed in an ultrasonic and heating water bath. The use of NH_4F was replaced with $NH_3 \cdot H_2O$ to neutralize the acid in the digestion reaction mixture. The experimental results showed that the oxidization digestion in an ultrasound-assisted system can be run in a lower acidic solution and neutralization with $NH_3 \cdot H_2O$ is not required. Thus the system is simplified as seen in Figure 1.

Reagents and Standard Solutions

All reagents were of analytical-reagent grade and double distilled water was used throughout.

A solution of glucose was used as the COD standard solution.

Stock solution of glucose (COD=500 mg L^{-1}) was prepared by dissolving 0.5160 g glucose in water, diluting to 1000-mL volume, then storing in a refrigerator.

Working solutions were prepared fresh daily by appropriately diluting the stock solution.

Potassium permanganate solution (2×10^{-3} mol L^{-1}) was prepared by dissolving 0.3161 g $KMnO_4$ in a 1000-mL brown volumetric flask and diluting to 1000-mL volume.

Hydrochloric acid solution was 3.0 mol L^{-1}.

Amberlite IRC-120 resin (Xi'an Electric Power Resin Plant, particle diameter 0.3–1.2 mm) was purified in a conventional way (25), then soaked in 10% hydrochloric acid solution for 24 h. After washing with water, the resin was filled into a micro-column.

Procedure

An analytical procedure consists of three processes: (a) digestion and on-line separation, (b) washing, and (c) elution and measurement.

When the injection valve is in the sampling position, the stream of the sample solution (S) first passes through a cation exchange micro-column (A) to remove the interferences of the cation ions, then merges with a stream of acidic $KMnO_4$ solution (R). The sample is oxidized, and MnO_4^- is reduced in the digestion reaction coil (L1) using ultrasound and heating. Passing through the cooling coil (L2), the Mn^{2+} produced by the reduction of MnO_4^- is adsorbed on-line on another cation exchange micro-column (B), which is connected to the injection valve by PTFE tubes as a sample loop, while anion MnO_4^- unreduced passes through micro-column (B) to waste. This is the digestion and on-line separation process (30 s).

When the valve is in the injection position, the first process consists of washing micro-column (B) for 30 s with water, then the Mn^{2+} is adsorbed on micro-column (B) is eluted by the HCl solution to the nebulizer, and measured by FAAS.

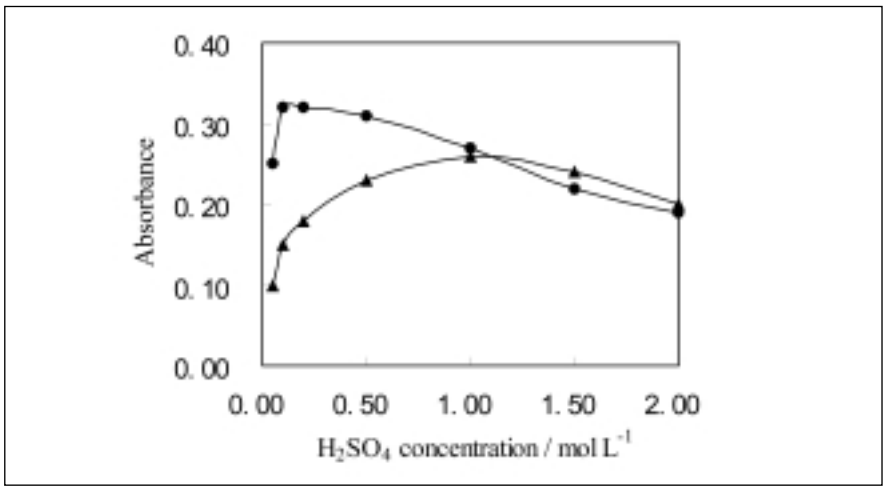

Fig. 2. The effect of acidity on sample digestion.
●—●, with ultrasound-assisted digestion (26.5 kHz, 600W);
▲—▲, without ultrasound-assisted digestion.

RESULTS AND DISCUSSIONS

Optimization of Solution pH for Mn^{2+} Adsorption

The solution pH value ranging from pH 1–7 was studied on the FI on-line adsorption of 0.5 mg L^{-1} Mn^{2+} on micro-column (B). The results showed that the optimum solution pH value for the adsorbing Mn^{2+} on micro-column (B) was between pH 2–3. It was found that a lower or higher pH was not beneficial to adsorption.

Digestion Condition Optimization

Digestion acidity, temperature, ultrasonic power, digestion coil, and concentration of potassium permanganate were taken as variables for the optimization of the digestion condition.

The effect of acidity on sample digestion with ultrasound (26.5KHz, 600W) and without ultrasound was investigated by adding different concentrations of H_2SO_4 to the potassium permanganate solution for the determination of 100 mg L^{-1} of COD, respectively. The results are shown in Figure 2. From these results, the following conclusions can be drawn: (a) the ultrasonic wave can advance the sample digestion at an acidity lower than 1.0 mol L^{-1} H_2SO_4; (b) the optimum acidity of ultrasound-assisted digestion is far lower than without ultrasound, the former being 0.1 mol L^{-1} of H_2SO_4 and latter being 1.0 mol L^{-1} of H_2SO_4; (c) ultrasonic digestion is more suitable to the determination of COD in a FIA system, because a lower acidity can lessen the corrosion of the system. Therefore, a potassium permanganate solution containing 0.1 mol L^{-1} of H_2SO_4 was used in this study. This acid concentration is far lower than required in all previous reports.

Temperature is an essential factor for most oxidation reactions. The influence of temperature on digestion was studied ranging from 20–90°C. The results show that the degree of digestion increased with a temperature up to 80°C; while above that temperature no significant increase was observed. The optimum digestion temperature for the ultrasonic wave and the heating water bath was set at 80°C.

The influence of ultrasonic power was investigated by adjusting the output power of the ultrasonic generator from 100–600 W at a fixed frequency of 26.5 KHz. As shown in Figure 3, the influence is slightly lower up to 200 W; then the digestion increases swiftly along with the measured absorbance with an increase in power from 200 to 500 W. Over 500 W, the influence remains virtually constant which most likely means that the digestion is complete. An ultrasonic power of 500 W was selected for this study. Using the acidity of 0.1 mol L^{-1} H_2SO_4, the digestion efficiency was tested once with ultrasound and once without ultrasound.

It was found that the ultrasonic wave declines quickly in plastics or rubber pipes (26). In order to avoid this absorbance, a glass pipe was chosen as the digestion reaction coil. At the time of the experiment, the glass digestion reaction coil was put into the ultrasonic and heating water bath. With an increase in the length of the digestion reaction coil (L1), the digestion time increases and the digestion reaction is more complete. With sample and acidic $KMnO_4$ solution flow rates of 5 mL min^{-1} and the glass digestion reaction coil above 500 cm, the digestion reaction is virtually complete. Thus, a 500-cm long glass digestion reaction coil (L1) was chosen.

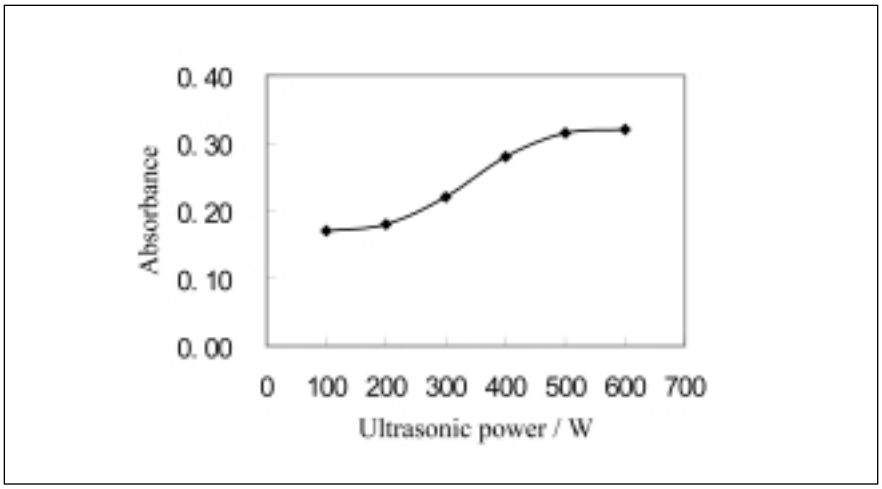

Fig. 3. The effect of ultrasonic power on sample digestion.

Potassium permanganate as an oxidizing reagent (rather than potassium dichromate) is more suitable in the FIA system for the determination of COD because it has a faster and higher oxidation ability and requires milder conditions such as in acidity. The experimental results showed that a potassium permanganate solution of 2.0×10^{-3} mol L^{-1} provides complete oxidation digestion of the sample.

Optimization of Elution Condition

The elution variables studied are type, concentration and flow rate of eluent, elution time, and mode.

The experimental results of hydrochloric acid, nitric acid, sodium chloride, and ammonium nitrate showed that hydrochloric acid was the best eluent due to its speed of elution and height of peak absorbance signal. The concentration of hydrochloric acid was tested ranging from 0.5–4.5 mol L^{-1}. The height of peak absorbance signal increased with an increase in hydrochloric acid concentration up to 3.0 mol L^{-1}; above that amount it remained constant. The eluent chosen was 3.0 mol L^{-1} of hydrochloric acid. The signal came back to baseline when the elution with 3.0 mol L^{-1} of hydrochloric acid was run for 120 s.

Increasing the flow rate of the eluent would be advantageous to the elution process, but not beneficial to FAAS measurement. The optimum flow rate chosen was 5 mL min^{-1}. The mode of reverse elution was the same as reported in our previous study (25).

Performance for COD Determination

Under optimum experimental conditions, the absorbance varies linearly with the concentration of COD in the range of 3–300 mg L^{-1}, and fits the equation: $A = 0.00296C + 0.0185$ ($r = 0.997$). The detection limit (DL) of 1 mg L^{-1} was calculated as three times the standard deviation of the absorbance for seven injections of the blank. The precision of the method obtained for nine samples containing 30 mg L^{-1} of COD was 2.7%, expressed as the relative standard deviation. The analytic throughput was found to be 24 samples per hour.

A lower DL value in comparison to the results from microwave digestion and FAAS detection (13,14) means that ultrasound-assisted digestion is more efficient than microwave digestion despite the milder conditions such as lower acid concentration and lower temperature.

Interferences

Chlorides cause the most important interferences in COD determination when potassium permanganate or potassium dichromate are used as the oxidizing reagent, since these can also be oxidized. Usually, the way of solving this problem is by adding $HgSO_4$ to the sample. The method developed by Hejzlar at el. (19) tolerates chloride concentrations up to 600 mg L^{-1} by adding an excess of Cr(III). Korenaga et al. (6) reported that when Ce(IV) is used as the oxidant, as high as 30,000 mg L^{-1} of chloride can be tolerated without adding $HgSO_4$. In our study, the interference from chloride was investigated for the determination of 100 mg L^{-1} COD. The results listed in Table I show that up to 1000 mg L^{-1} of chloride can be tolerated without adding $HgSO_4$.

When using ultrasonic digestion with on-line ion exchange separation and FI-FAAS for the determination of COD, another problem to be considered is that a too high cation concentration in a sample might affect the adsorption of Mn^{2+} on micro-column (B). To avoid this interference, the sample was first passed through cation exchange micro-column (A) before reaction with the oxidizing agent.

TABLE I
Effect of Chloride Concentration on COD Determination

COD (mg L^{-1})	Cl^- (mg L^{-1})	A	COD (found) (mg L^{-1})	Error (%)
100	0	0.314	99.8	–0.2
100	50	0.310	98.5	–1.5
100	100	0.317	100.8	0.8
100	500	0.319	101.5	1.5
100	1000	0.321	102.2	2.2
100	5000	0.343	109.6	9.6
100	10,000	0.389	125.2	25.2

TABLE II
Results of COD Determination in Real Samples

Sample	COD (mg L^{-1})[a]		Error (%)
	Proposed Method	Standard Method	
Well Water	11.1	11.6	–4.3
River Water	47.2	46.3	1.9
Pool Water I	84.1	85.9	–2.1
Pool Water II	49.2	48.9	0.6

[a] Average of three determinations.

Application

To investigate the applicability of the method described to real samples, the COD was determined in well, river, and pool water samples. After filtering, each sample was anlayzed directly and the results are given in Table II. Also listed are the results obtained by the conventional and standard methods with potassium dichromate. Application of the statistical *t* test assured that the results of both methods shows no significant difference up to a confidence level of 95%.

CONCLUSION

An ultrasound-assisted digestion method for the COD determination combined with a flow injection system is described in which Mn^{2+} produced by the reduction of MO_4^- is separated on-line with a cation exchange micro-column and determined by FAAS. This method proves to be an effective way for the determination of COD and offers lower digestion acidity, shorter digestion time, higher throughput, lower detection limit and interference, simpler operation, and better precision in comparison to other reported methods. It would be desirable to investigate the applicability of this approach further by applying it to the analysis of different types of water samples, for using it in the process control of wastewater treatment, and for quality management of environmental waters.

Received August 11, 2003.

REFERENCES

1. Association of Official Analytical Chemists, Official Methods of Analysis, Virginia, USA, 15th ed., 317 (1990).
2. The Society for Analytical Chemistry, Official, Standardised and Recommended Methods of Analysis, London, UK, 2nd ed., 383 (1973).
3. T. Korenaga, Anal. Lett. 13, 1001 (1980).
4. T. Korenaga, H. Ikatsu, Analyst 106, 653 (1981).
5. T. Korenaga, H. Ikatsu, Anal. Chim. Acta 141, 301 (1982).
6. T. Korenaga, X. Zhou, O. Kimiko, T. Moriwake, Anal. Chim. Acta, 272, 237 (1993).
7. J.M.H. Appleton, J.F. Tyson, R.P. Mounce, Anal. Chim. Acta 179, 269 (1986).
8. M.L. Balconi, F. Sigon, M. Borgarello, R. Ferraroli, F. Realini, Anal. Chim. Acta 234, 167 (1990).
9. B.V. Pecharroman, A.I. Reina, M.D.L. Castro, Analyst 124, 1261 (1999).
10. L.-C. Tian, S.-M. Wu, Anal. Chim. Acta 261, 301 (1992).
11. M.L. Balconi, M. Borgarello, R. Ferraroli, Anal. Chim. Acta 261, 295 (1992).
12. D. Rodreva, Z. Areva, Anal. Lab. 3 (3), 183 (1994).
13. A. Cuesta, J.L. Todoli, A. Canals, Spectrochim. Acta, Part B 51, 1791 (1996).
14. A. Cuesta, J.L. Todoli, A. Canals, Anal. Chim. Acta 372, 399 (1998).
15. A.-G. Zhong, PTCA (Part B: Chem. Anal.) (in Chinese) 37, 412 (2001).
16. K.H. Lee, T. Ishikawa, S. McNiven, Y. Nomura, S. Sasaki, Y. Arikawa, I. Karube, Anal. Chim. Acta 386, 211 (1999).
17. Y.-C. Kim, K.-H. Lee, S. Sasaki, K. Hashimoto, K. Ikebukuro, I. Karube, Anal. Chem. 72, 3379 (2000).
18. Y.-C. Kim, S. Sasaki, K. Yano, K. Ikebukuro, K. Hashimoto, I. karube, Anal. Chim. Acta 432, 59 (2001).
19. J. Hejzlar, J. kopacek, Analyst 115, 1463 (1990).
20. D.-Z. Dan, Anal. Chim. Acta 420, 39 (2000).
21. J.P. Lorimer, T.J. Mason, Chem. Soc. Rev. 16, 239 (1987).
22. B. Ashlsh, H.M. Cheung, Environ. Sci. Technol. 28 (8), 1481 (1994).
23. C.W. James, T. Junk, Waste Manag. 15, 303 (1995).
24. J. Hofmanm, D. Hantzschel, UFZ-Ber 23, 49 (2000).
25. Z.-Q. Zhang, Y.-C. Jiang, H.-T. Yan, At. Spectrosc. 24 (1), 27 (2003).
26. K. Gabriel, S. Petrie, Annu Tech Conf-Soc Plast. 58 (2), 1489 (2000).

Atomic Spectroscopy
Vol. 25(4), July/August 2004

Printed in the United States and published six times a year by:

PerkinElmer Life and
Analytical Sciences
710 Bridgeport Avenue
Shelton, CT 06484-4794 USA
www.perkinelmer.com

SUBSCRIPTION INFORMATION

Atomic Spectroscopy
P.O. Box 3674
Barrington, IL 60011 USA
Fax: +1 (847) 304-6865

2004 Subscription Rates

- U.S. $60.00 includes third-class mail delivery worldwide; $20.00 extra for electronic file.
- U.S. $80.00 includes airmail delivery; $20 extra for electronic file.
- U.S. $60.00 for electronic file only.
- Payment by check (drawn on U.S. bank in U.S. funds) made out to: "*Atomic Spectroscopy*"

Electronic File

- For electronic file, send request via e-mail to: atsponline@yahoo.com

Back Issues/Claims

- Single back issues are available at $15.00 each.
- Subscriber claims for missing back issues will be honored at no charge within 90 days of issue mailing date.

Address Changes to:
Atomic Spectroscopy
P.O. Box 3674
Barrington, IL 60011 USA

Microfilm

Atomic Spectroscopy issues are available from:
University Microfilms International
300 N. Zeeb Road
Ann Arbor, MI 48106 USA
Tel: (800) 521-0600 (within the U.S.)
+1 (313) 761-4700 (internationally)

Guidelines for Authors

Atomic Spectroscopy serves as a medium for the dissemination of general information together with new applications and analytical data in atomic absorption spectrometry.

The pages of *Atomic Spectroscopy* are open to all workers in the field of atomic spectroscopy. There is no charge for publication of a manuscript.

The journal has around 1500 subscribers on a worldwide basis, and its success can be attributed to the excellent contributions of its authors as well as the technical guidance of its reviewers and the Technical Editors.

The original of the manuscript should be submitted to the editor by mail plus electronic file on disk or e-mail in the following manner:

1. Mail original of text, double-spaced, plus graphics in black/white.
2. Provide text and tables in .doc file and figures in doc or tif files.
3. Number the references in the order they are cited in the text.
4. Submit original drawings or glossy photographs and figure captions.
5. Consult a current copy of *Atomic Spectroscopy* for format.
6. Or simply e-mail text and tables in doc file and graphics in doc or tif files to the editor: anneliese.lust@perkinelmer.com or annelieselust@aol.com

All manuscripts are sent to two reviewers. If there is disagreement, a third reviewer is consulted.

Minor changes in style are made in-house and submitted to the author for approval.

A copyright transfer form is sent to the author for signature.

If a revision of the manuscript is required before publication can be considered, the paper is returned to the author(s) with the reviewers' comments.

In the interest of speed of publication, a pdf file of the type-set text is e-mailed to the corresponding author before publication for final approval.

Additional reprints can be purchased, but the request must be made at the time the manuscript is approved for publication.

Anneliese Lust
Editor, *Atomic Spectroscopy*
PerkinElmer
Life and Analytical Sciences
710 Bridgeport Avenue
Shelton, CT 06484-4794 USA

Atomic Absorption

Just touch and go.

There, that's all the training you need.

Walk up to the AAnalyst 200 and let the touch screen guide you through everything from setup to analysis. It practically tells you what to do—and in your own language. All instrument controls are right there on the screen, available at your fingertips. Even troubleshooting and repairs are easier, with quick-change parts you simply snap out and snap in. No service visit, no down time. As rugged and reliable as ever, our newest AAnalyst is a better way to do AA. Experience it for yourself. Talk to a PerkinElmer inorganic analysis specialist today.

PerkinElmer®
precisely.

ISO 9001 CERTIFIED

U.S. 800-762-4000 (+1) 203-925-4600

www.perkinelmer.com

007055_04